Lattice determination of the HVP NLO contributions to the $(g-2)_\mu$

Arnau Beltran & Hartmut Wittig

MPA retreat
30^{th} of September 2024

Table of contents

Motivation and current muon g-2 status

Magnetic field couples to the spin of a charged lepton through the g factor

$$\mathcal{H}_l = \vec{\mu}_l \cdot \vec{B} \qquad \vec{\mu}_l = \mathbf{g}_l \frac{q_l}{2m_l}\vec{S}$$

Dirac theory predicts $g = 2$ for spin 1/2 particles at first order, quantum effects shift this value to $g > 2$. This difference is known as the anomalous magnetic moment of the lepton.

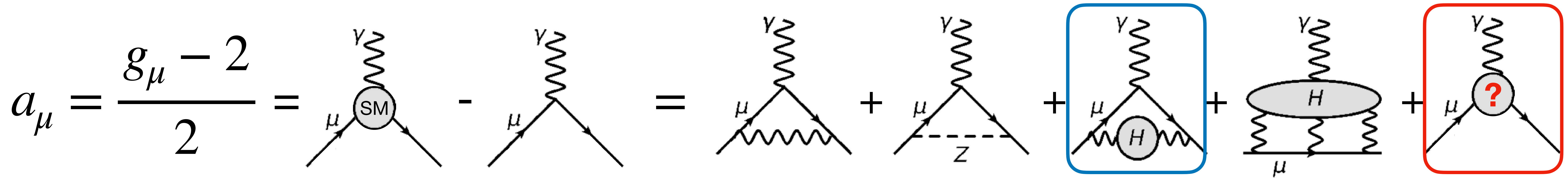

PD Dr. Tobias Huber; October 13, 2021

Most contributing to the total uncertainty for $l = \mu$ and probably for $l = e$ in the near future

Precise exp. and th. predictions (picture in 2020)

Northwestern 2023, Fermilab 2023 $a_\mu^{\text{exp}} = 116592059(22) \times 10^{-11}$

WP. 2020 $a_\mu^{\text{th}} = 116591810(43) \times 10^{-11}$

} 5.2σ discrepancy

Plenty of new results and discoveries since then; new more precise lattice results have changed the way we look at this. $\Longrightarrow$ **Big discrepancies between lattice and data driven approaches**

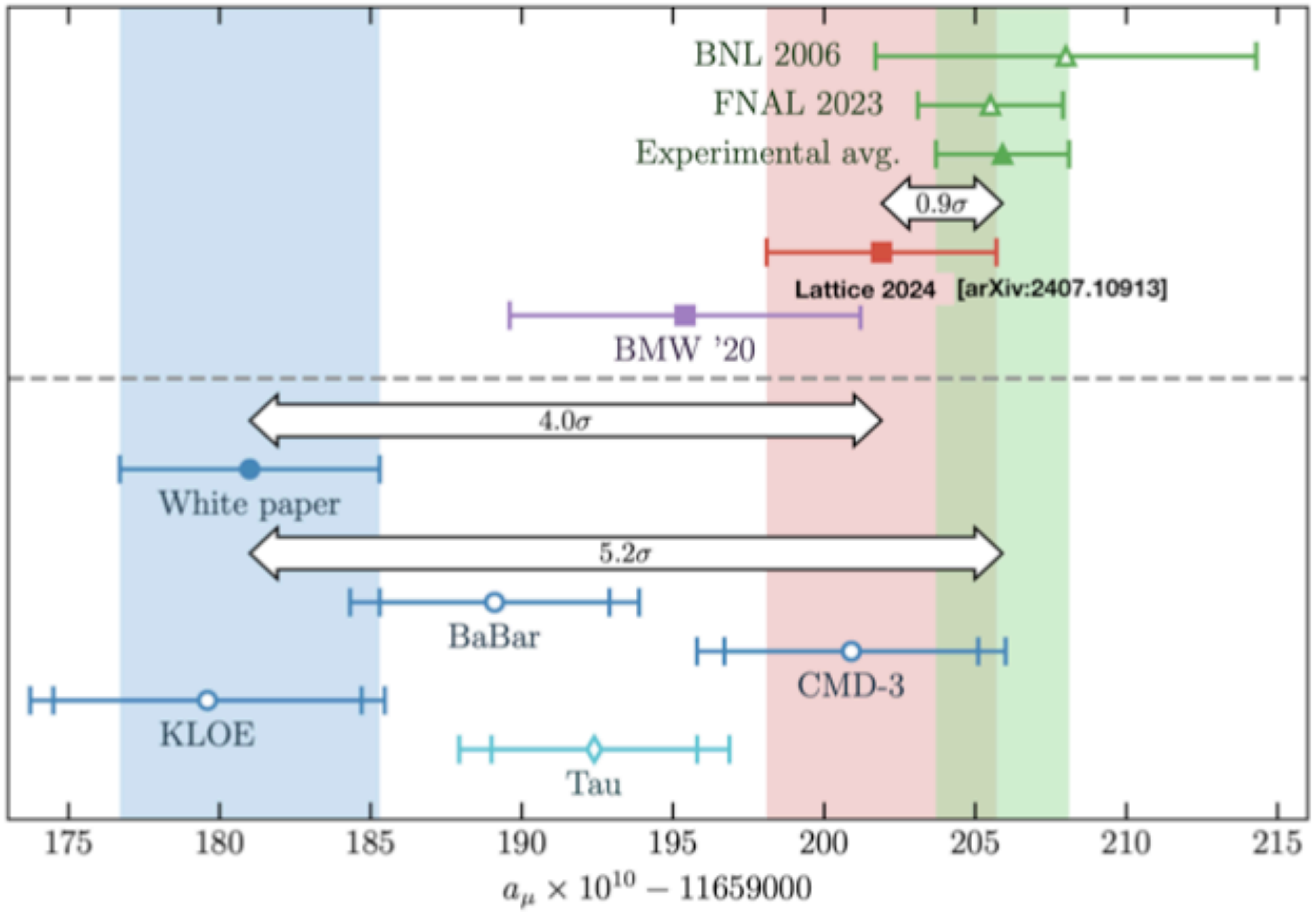

Anna Driutti, Lecture 1: Muon Magnetic Moment Experiments

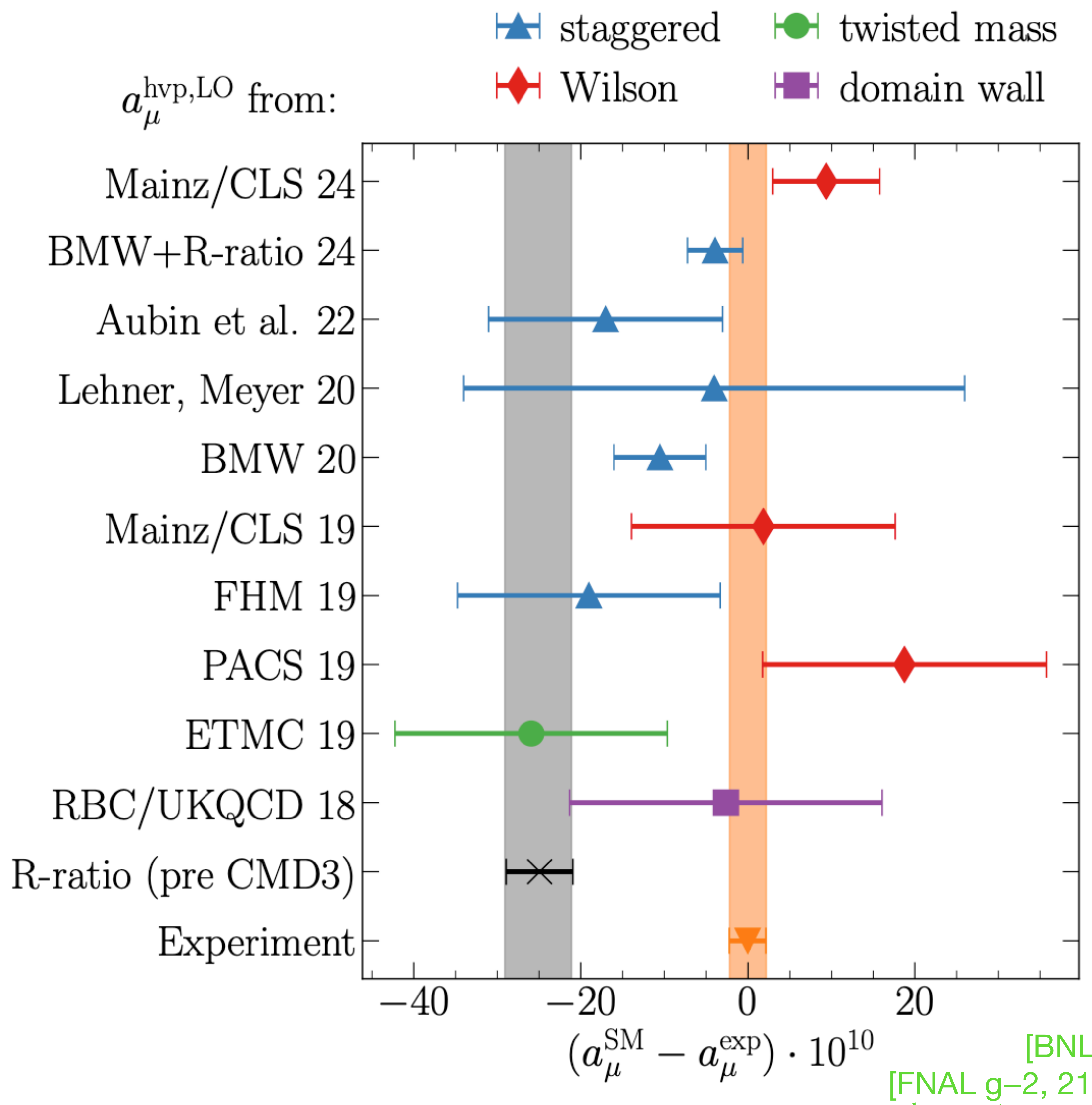

[BNL g–2, hep-ex/0602035]
[FNAL g–2, 2104.03281, 2308.06230]
Simon Kuberski, Update from Mainz on $a_\mu^{\rm hvp}$, 7th plenary workshop muon g-2

a_μ^{hvp} structure

LO & NLO contributions to the a_μ^{hvp}

E.g. in the LO case:

$\hat{q} = \frac{q}{m_\mu}$

$a_\mu^{\text{hvp}}[\text{LO}] =$

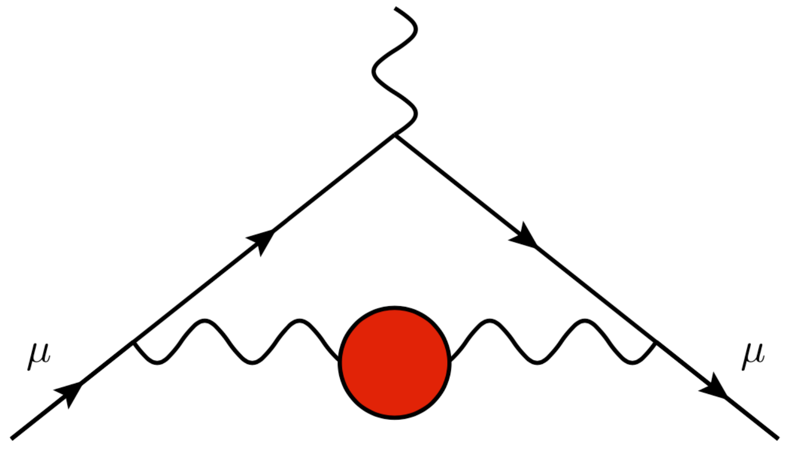

$= \int_0^\infty dq^2$

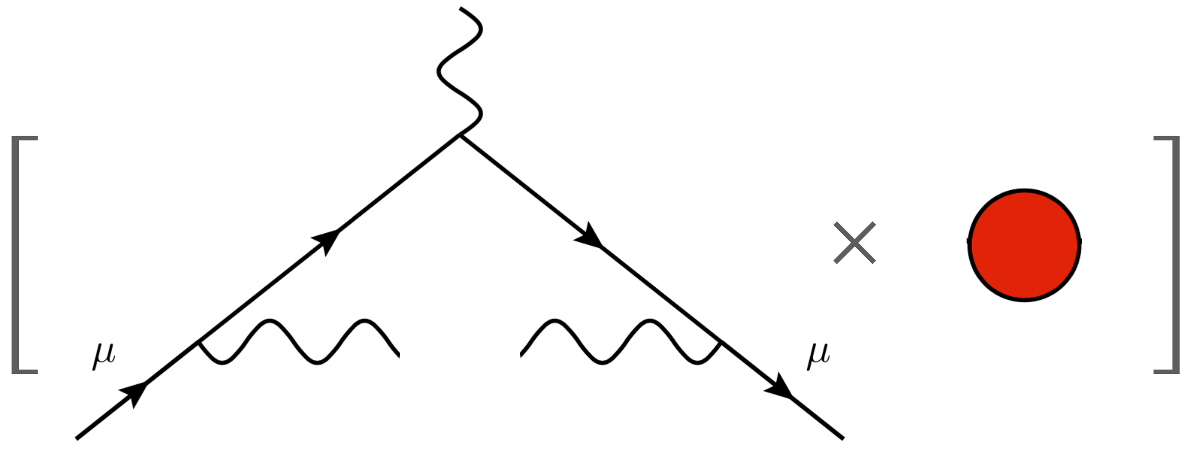

$= \int_0^\infty dq^2 \, f^{(\text{LO})}(\hat{q}^2) \, \hat{\Pi}(q^2)$

Kernel: QED structure of the diagram, known analytic (∼ weight) function

Hadron Vacuum Polarisation (HVP) function: Includes all the **QCD** effects → **non-perturbative** nature, must be computed by other means

M. Passera et al. Physics Letters B 834 (2022) 137462

$a_\mu^{\rm hvp}$ structure

$\hat{q} = \frac{q}{m_\mu}$

E.g. in the LO case:

$a_\mu^{\rm hvp}[\rm LO] =$

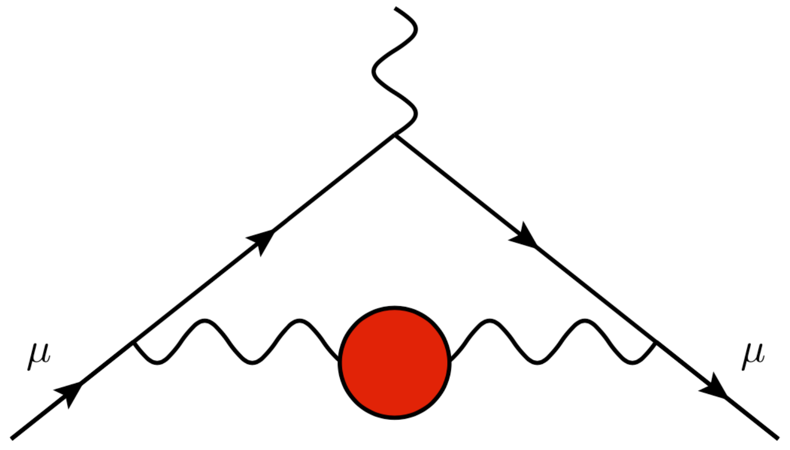

$= \int_0^\infty dq^2 \Big[$

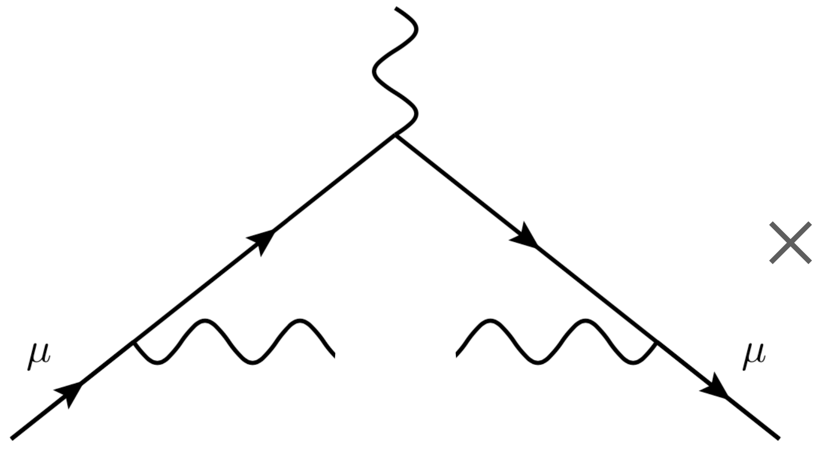

$\times$

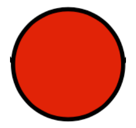

$\Big] = \int_0^\infty dq^2 \; f^{(\rm LO)}(\hat{q}^2)\; \hat{\Pi}(q^2)$

E.g. photon and muon corrections in the NLO case:

$a_\mu^{\rm hvp}[\rm NLO_a] =$

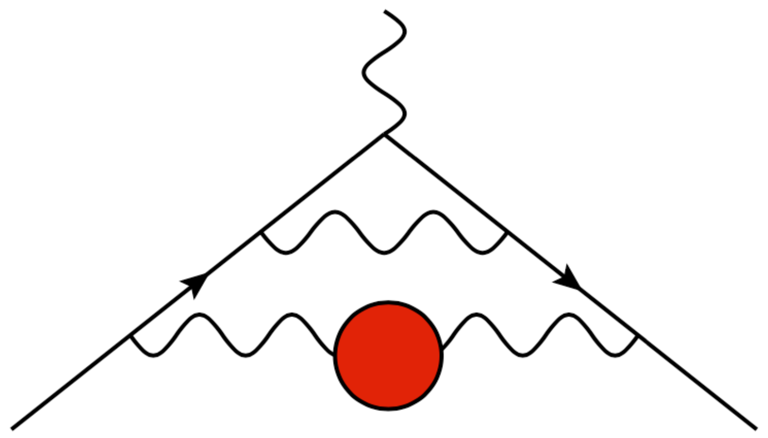

$= \int_0^\infty dq^2 \Big[$

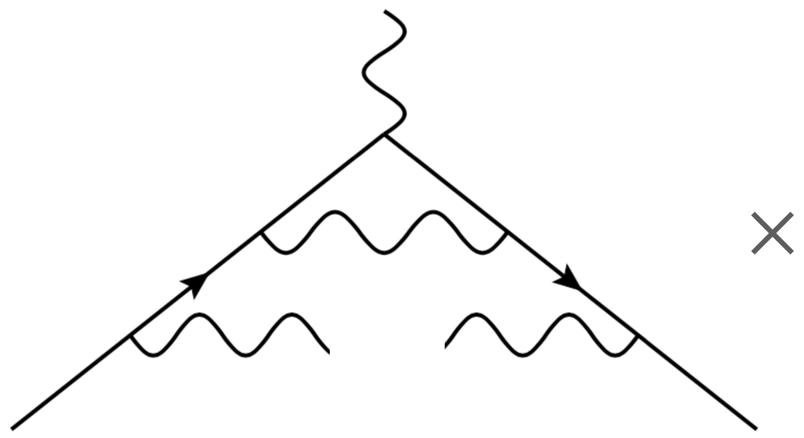

$\times$

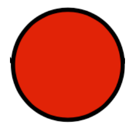

$\Big] = \int_0^\infty dq^2 \; f^{(\rm NLO_a)}(\hat{q}^2)\; \hat{\Pi}(q^2)$

M. Passera et al. Physics Letters B 834 (2022) 137462

LO & NLO contributions

LO contribution:

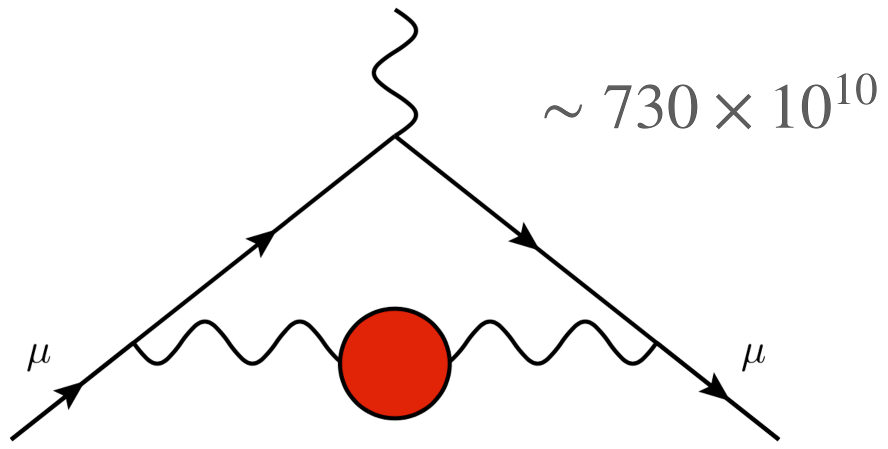

NLO contribution:

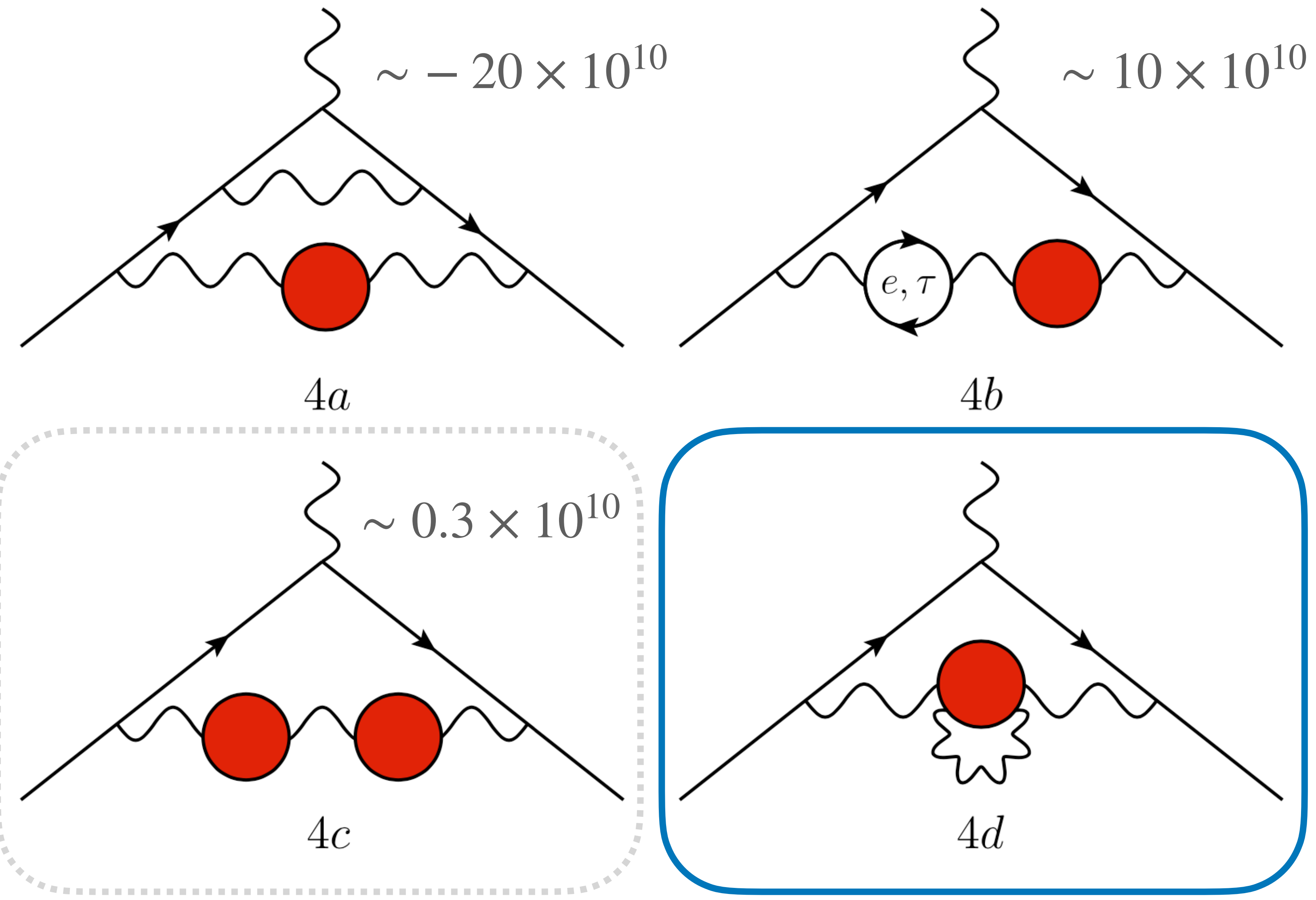

Involved, in lattice QCD it's usually computed as a small correction of the LO

M. Passera et al. Physics Letters B 834 (2022) 137462

Generally can be expressed as the integral of the Kernel $f(q^2)$ (given by the QED structure) times the HVP $\hat{\Pi}(q^2)$

$$a_\mu^{\text{hvp}}[(i)] = \left(\frac{\alpha}{\pi}\right)^{\geq 2} \int_0^\infty dq^2 \; f^{(i)}(\hat{q}^2)\hat{\Pi}(q^2) \text{ with } i = \text{LO, NLO}_\text{a}\text{, NLO}_\text{b}$$

e.g. $f^{(\text{NLO}_\text{b})} = 2\, f^{(\text{LO})} \times F_l$.

$$a_\mu^{\text{hvp}}[(\text{NLO}_\text{c})] = \left(\frac{\alpha}{\pi}\right)^3 \int_0^\infty dq^2 \; f^{(\text{LO})}(\hat{q}^2)\left[\hat{\Pi}(q^2)\right]^2$$

PROBLEM:

non-perturbative QCD effects → $\hat{\Pi}(q^2)$ **cannot** be computed with perturbation theory!

a_μ^{hvp} from lattice simulations

$\hat{\Pi}(q^2)$ must be found non-perturbatively.

HVP tensor: $$i\Pi^{\mu\nu}(q) = i\left(g^{\mu\nu}q^2 - q^\mu q^\nu\right)\Pi(q^2) = \int d^4x e^{iq\cdot x}\langle j^\mu_{\text{em}}(x) j^\nu_{\text{em}}(0)\rangle$$

Lattice correlator: $$G(\tau) = -\frac{1}{3}\sum_{\vec{x}\in\Lambda}\sum_{k=0}^{3}\langle j^k_{\text{em}}(\vec{x},\tau) j^k_{\text{em}}(0)\rangle$$ ← This can be computed in the lattice

There's an analytic relation between both descriptions: D.Berneckerand H.B.Meyer. 2011. Eur. Phys.

$$\hat{\Pi}(\omega^2) = \frac{4\pi^2}{\omega^2}\int_0^\infty dt\ G(t)\left[\omega^2 t^2 - 4\sin^2\frac{\omega t}{2}\right]$$

Same idea as before applies, energy integral is absorbed by the Kernel and a_μ^{hvp} is expressed as an integral over Euclidian time.

$\hat{\omega} = \frac{\omega}{m_\mu}$, $\hat{t} = m_\mu t$, $\hat{f} = m_\mu^2 f$

$$a_\mu^{\text{hvp}}[(i)] = \left(\frac{\alpha}{\pi}\right)^{\geq 2}\int_0^\infty dt\ \tilde{f}^{(i)}(t) G(t)$$ with $$\tilde{f}^{(i)}(t) = 8\pi^2\int_0^\infty \frac{d\hat{\omega}}{\hat{\omega}}\hat{f}^{(i)}(\hat{\omega}^2)\left[\hat{\omega}^2\hat{t}^2 - 4\sin^2\frac{\hat{\omega}\hat{t}}{2}\right]$$ for $i = \text{LO}, \text{NLO}_\text{a}, \text{NLO}_\text{b}$

We need to find a suitable representation for these kernels!!

TMR Kernels

LO

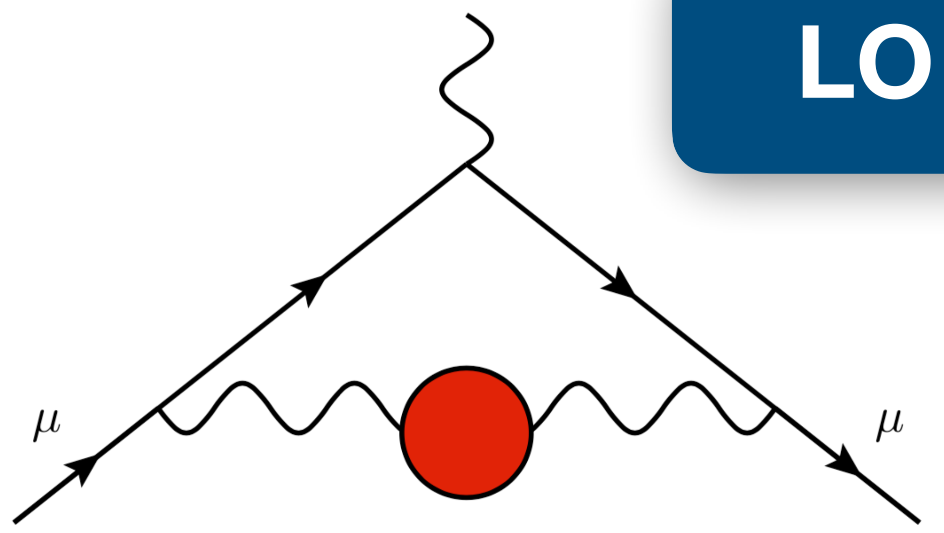

$$\tilde{f}^{(\text{LO})}(t) = \frac{8\pi^2}{m_\mu^2}\int_0^\infty \frac{d\hat{\omega}^2}{\hat{\omega}^2}\hat{f}^{(\text{LO})}(\hat{\omega}^2)\left[\hat{\omega}^2\hat{t}^2 - 4\sin^2\frac{\hat{\omega}\hat{t}}{2}\right] \qquad \hat{f}^{(\text{LO})}(s) = \frac{1}{2}\left(\sqrt{s(s+4)} - s\right) + \frac{1}{\sqrt{s(s+4)}} - 1$$

Has a closed-form solution.

$$\tilde{f}^{(\text{LO})}(t) = \frac{2\pi^2}{m_\mu^2}\left(-2 + 8\gamma_E + \frac{4}{\hat{t}^2} + \hat{t}^2 - \frac{8}{\hat{t}}K_1(2\hat{t}) + 8\ln(\hat{t}) + G^{2,1}_{1,3}\left(\hat{t}^2 \middle| \begin{matrix} \frac{3}{2} \\ 0,1,\frac{1}{2}\end{matrix}\right)\right)$$

Suitable representation of the kernel to combine it with lattice data

$\hat{t} \to 0$

$$\frac{m_\mu^2}{16\pi^2}\tilde{f}^{(\text{LO})}(t) = \begin{cases} \sum_{n=4, n\in\text{even}}^{N} \frac{a_n + b_n(\gamma_E + \ln\hat{t})}{n!}\hat{t}^n & \hat{t} \le \hat{t}^* \\ \frac{\hat{t}^2}{8} - \frac{\pi}{4}\hat{t} + \ln(\hat{t}) + \gamma_E - \frac{1}{4} + \frac{1}{2\hat{t}^2} + \sqrt{\frac{\pi}{t}}e^{-2\hat{t}}\sum_{p=0}^{P} a_p^{(b)}\left(\frac{\hat{t}_0}{\hat{t}} - 1\right)^p & \hat{t} > \hat{t}^* \end{cases}$$

$\hat{t} \to \infty$

Suppressed $\hat{t} \sim \hat{t}_0$

The hadronic vacuum polarization contribution to the muon g – 2 from lattice QCD. 2017. M. Della Morte et al

TMR Kernels

$$\tilde{f}^{(\text{NLO}_a)}(t) = \frac{8\pi^2}{m_\mu^2}\int_0^\infty \frac{d\hat{\omega}^2}{\hat{\omega}^2}\hat{f}^{(\text{NLO}_a)}(\hat{\omega}^2)\left[\hat{\omega}^2\hat{t}^2 - 4\sin^2\frac{\hat{\omega}\hat{t}}{2}\right]$$

$$\hat{f}^{(\text{NLO}_a)}(s) = \frac{2F_4\left(\frac{1}{y(-s)}\right)}{-s}$$ where $$y(z) = \frac{z-\sqrt{z(z-4)}}{z+\sqrt{z(z-4)}}$$ and :

$$F_4(u) = \frac{23u^6 - 37u^5 + 124u^4 - 86u^3 - 57u^2 + 99u + 78}{72(u-1)^2u(u+1)} + \frac{\left(12u^8 - 11u^7 - 78u^6 + 21u^5 + 4u^4 - 15u^3 + 13u + 6\right)\log(-u)}{12(u-1)^3u(u+1)^2}$$

$$+\frac{\left(-7u^4 - 8u^3 + 8u + 7\right)\log(1-u)}{12u^2} + \frac{(u+1)\left(-u^3 + 7u^2 + 8u + 6\right)\log(u+1)}{12u^2}$$

$$\frac{\left(-3u^4 - 5u^3 - 7u^2 - 5u - 3\right)\left(2\text{Li}_2(-u) + 4\text{Li}_2(u) + \log(-u)\log\left((1-u)^2(u+1)\right)\right)}{6u^2}$$

NLOa

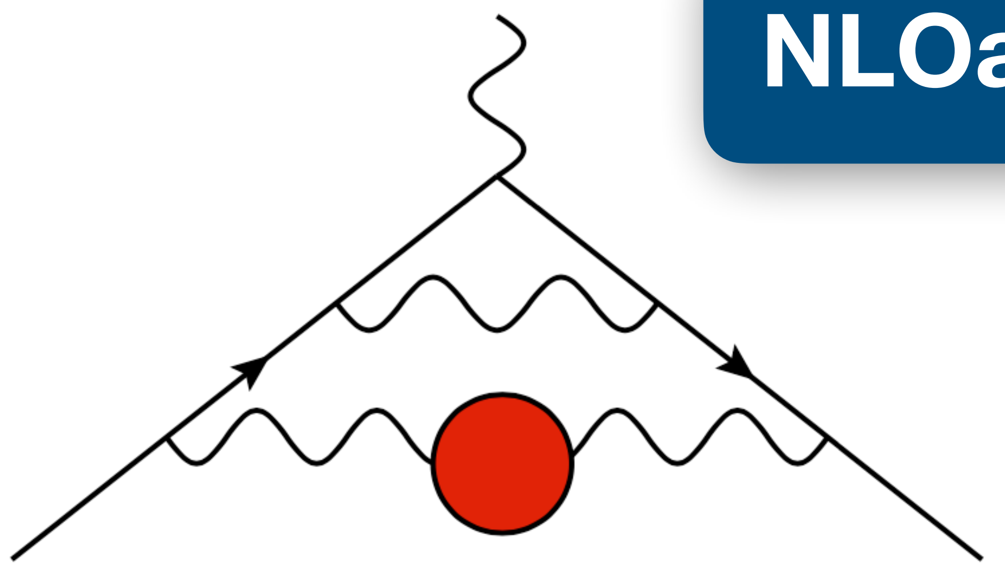

NO CLOSED-FORM SOLUTION

NLOa

$$\tilde{f}^{(\mathrm{NLO_a})}(t) = \frac{8\pi^2}{m_\mu^2}\int_0^\infty \frac{d\hat{\omega}^2}{\hat{\omega}^2}\hat{f}^{(\mathrm{NLO_a})}(\hat{\omega}^2)\left[\hat{\omega}^2\hat{t}^2 - 4\sin^2\frac{\hat{\omega}\hat{t}}{2}\right]$$

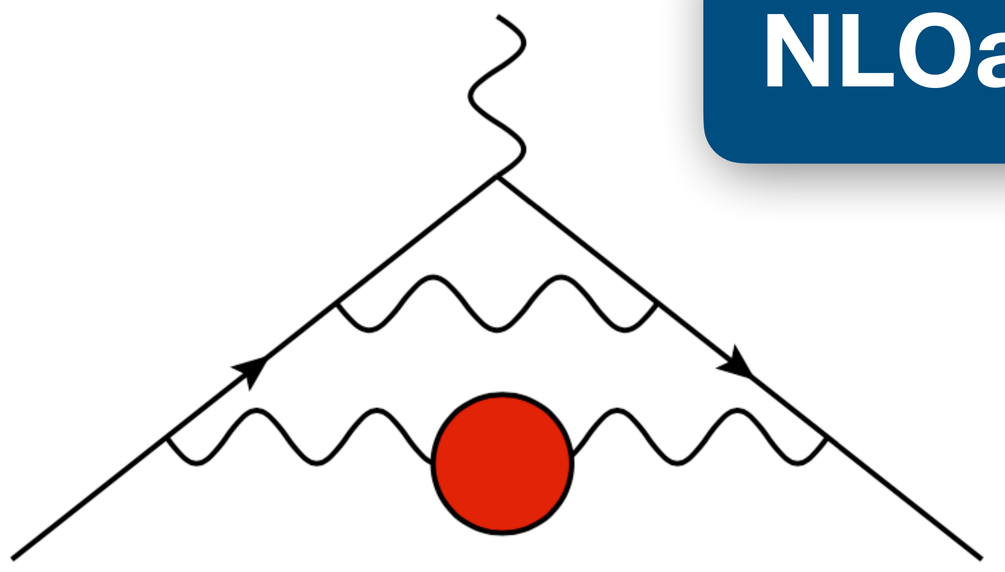

NO closed-form solution.

For $\hat{t} \ll 1$ one can proceed as:

$$\int_0^\infty \frac{d\hat{\omega}^2}{\hat{\omega}^2}\hat{f}^{(\mathrm{NLO_a})}(\hat{\omega}^2)\left[\hat{\omega}^2\hat{t}^2 - 4\sin^2\frac{\hat{\omega}\hat{t}}{2}\right] = \int_0^{\frac{1-\hat{t}}{\sqrt{\hat{t}}}} \frac{d\hat{\omega}^2}{\hat{\omega}^2}\hat{f}^{(\mathrm{NLO_a})}(\hat{\omega}^2)\underbrace{\left[\hat{\omega}^2\hat{t}^2 - 4\sin^2\frac{\hat{\omega}\hat{t}}{2}\right]}_{\hat{\omega}\hat{t}\sim 0} + \int_{\frac{1-\hat{t}}{\sqrt{\hat{t}}}}^\infty \frac{d\hat{\omega}^2}{\hat{\omega}^2}\underbrace{\hat{f}^{(\mathrm{NLO_a})}(\hat{\omega}^2)}_{\hat{\omega}\sim\infty}\left[\hat{\omega}^2\hat{t}^2 - 4\sin^2\frac{\hat{\omega}\hat{t}}{2}\right]$$

For $\hat{t} \gg 1$ one solves analytically as much as possible and rotates the cosine to the complex plane to make it real and thus make explicit the suppressed contribution. Then, one numerically expands around $\hat{t}_0$ by studying the asymptotic behavior of each piece.

$$\frac{m_\mu^2}{16\pi^2}\tilde{f}^{\mathrm{NLO_a}}(t) = \begin{cases} \sum_{n=4,n\in\mathrm{even}}^{N} \frac{a_n + b_n\pi^2 + c_n(\gamma_E + \ln\hat{t}) + d_n(\gamma_E+\ln\hat{t})^2}{n!}\hat{t}^n & \hat{t} \le \hat{t}^* \\ \text{Dominant}[\propto \hat{t}^2] + \sum_{p=0}^{P}\left[\left(\frac{a_p^{(b;1;1)}}{\hat{t}} + \frac{a_p^{(b;1;2)}}{\hat{t}^2}\right)\left(\frac{\hat{t}_0^2}{\hat{t}^2}-1\right)^p + e^{-2\hat{t}}\left(a_p^{(b;2;1)} + \frac{a_p^{(b;2;2)}\ln\hat{t} + a_p^{(b;2;3)}}{\sqrt{\hat{t}}}\right)\left(\frac{\hat{t}_0}{\hat{t}}-1\right)^p\right] & \hat{t} > \hat{t}^* \end{cases}$$

With $N = 30$ and $P = 12$, $\hat{t}^* = 3.82$ and $\hat{t}_0 = 5$ a precision $< 3\times 10^{-8}$ $\forall\ \hat{t}$ is achieved.

Time-kernel for lattice determinations of NLO hadronic vacuum polarisation contributions to the muon g-2. 2024. S. Laporta et al.

TMR Kernels

NLOb

$$\tilde{f}^{(\mathrm{NLO_b})}(t) = \frac{8\pi^2}{m_\mu^2}\int_0^\infty \frac{d\hat\omega^2}{\hat\omega^2} 2\hat{f}^{(\mathrm{LO})}(\hat\omega^2) F_e(\hat\omega^2, M)\left[\hat\omega^2\hat t^2 - 4\sin^2\frac{\hat\omega\hat t}{2}\right];\quad F^l(\omega^2; m_l^2) = -\frac{8}{9}+\frac{\beta^2}{3}-\left(\frac{1}{2}-\frac{\beta^2}{6}\right)\beta\ln\frac{\beta-1}{\beta+2};\quad \beta=\sqrt{1+4\frac{m_l^2}{\omega^2}}$$

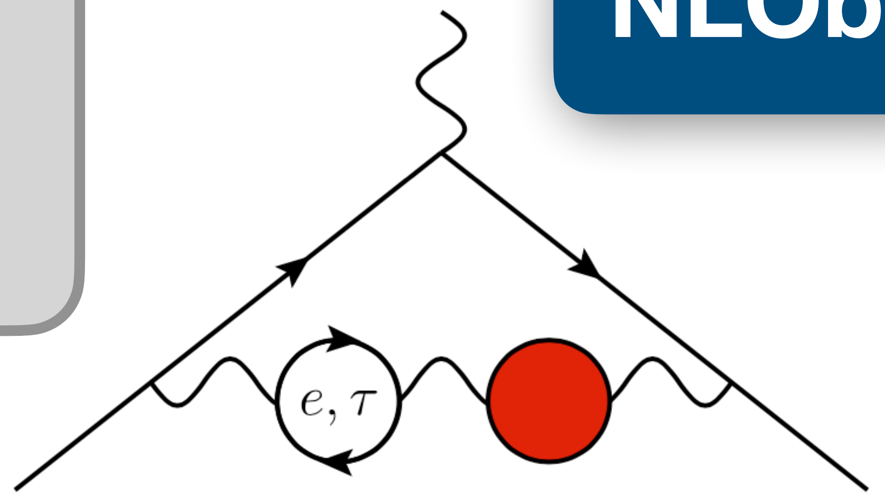

NO closed-form solution.

We have a new parameter $M = m_e/m_\mu \ll 1$, for $\hat t \ll 1$.

$$\int_0^{\frac{\sqrt{M}}{1-M}} \frac{d\hat\omega^2}{\hat\omega^2} \underbrace{\hat f^{(\mathrm{LO})}(\hat\omega^2)}_{\hat\omega\sim 0} F_l(\omega^2; M) \underbrace{\left[\hat\omega^2\hat t^2 - 4\sin^2\frac{\hat\omega\hat t}{2}\right]}_{\hat\omega\hat t\sim 0} + \int_{\frac{\sqrt{M}}{1-M}}^{\frac{1-\hat t}{\sqrt{\hat t}}} \frac{d\hat\omega^2}{\hat\omega^2} \hat f^{(\mathrm{LO})}(\hat\omega^2) \underbrace{F_l(\omega^2; M)}_{M\sim 0} \underbrace{\left[\hat\omega^2\hat t^2 - 4\sin^2\frac{\hat\omega\hat t}{2}\right]}_{\hat\omega\hat t\sim 0} + \int_{\frac{1-\hat t}{\sqrt{\hat t}}}^{\infty} \frac{d\hat\omega^2}{\hat\omega^2} \underbrace{\hat f^{(\mathrm{LO})}(\hat\omega^2)}_{\hat\omega\sim\infty} \underbrace{F_l(\omega^2; M)}_{M\sim 0} \left[\hat\omega^2\hat t^2 - 4\sin^2\frac{\hat\omega\hat t}{2}\right]$$

Same procedure for $\hat t \gg 1$ as before, now two exp. surpassed behaviors have to be taken into account!

$$\frac{m_\mu^2}{16\pi^2}\tilde f^{\mathrm{NLO_b}}(t) = \begin{cases} \sum_{n=4,\ n\in\text{even}}^{N} \sum_{m=0}^{M} \left[a_{nm} + b_{nm}\pi^2 + c_{nm}\left(\gamma_E + \ln\hat t\right) + d_{nm}\left(\gamma_E+\ln\hat t\right)^2\right]\frac{\hat t^n}{n!}M^m & \hat t \le \hat t^* \\ \text{Dominant}[\propto \hat t^2] + \sum_{p=0}^{P}\left[\frac{a_p^{(b;1;2)}}{\hat t^2}\left(\frac{\hat t_0^2}{\hat t^2}-1\right)^p + \left(\frac{e^{-2\hat t}}{\sqrt{\hat t}}a_p^{(b;2;3)} + \frac{e^{-2M\hat t}}{\sqrt{\hat t}}a_p^{(b;2;4)}\right)\left(\frac{\hat t_0}{\hat t}-1\right)^p\right] & \hat t > \hat t^* \end{cases}$$

Up to $N = 32$ and $M = 6$ coefficients have been extracted to achieve a precision $< 10^{-8}$ for $\hat t < \hat t^* = 4$.
$\hat t \gg 1$ suppressed contribution is still being worked around; terms with $e^{-2M\hat t}$ asymptotic behavior provide a new layer of difficulty to the problem.

TMR Kernels

a_μ^{hvp} from lattice simulations

n	$m=0$	$m=2$	$m=4$	$m=6$
4	$-\frac{2}{9}\ln M-\frac{1}{18}$	1	$4+4\ln^2 M$	$-\frac{46}{27}+\frac{28\ln M}{9}-\frac{1}{3}8\ln^2 M$
6	$\frac{169\ln M}{90}-\frac{36931}{10800}$	$-\frac{2}{3}$	$-2-2\ln M$	$\frac{80}{27}+\frac{56\ln M}{9}+\frac{16\ln^2 M}{3}$
8	$\frac{1604\ln M}{105}-\frac{210047}{8820}$	$\frac{704}{105}$	$-\frac{10}{9}+\frac{2}{3}\ln M$	$-\frac{-38}{9}-\frac{8\ln M}{3}$
10	$\frac{11018\ln M}{135}-\frac{21513067}{170100}$	$\frac{5344}{105}$	$\frac{17550779}{396900}-\frac{4756\ln M}{315}$	$-\frac{4}{9}+\frac{16\ln M}{9}$
12	$\frac{29412\ln M}{77}-\frac{2894965393}{4802490}$	$\frac{130858}{495}$	$\frac{1206809563}{4002075}-\frac{127228\ln M}{1155}$	$\frac{1883184914}{36018675}-\frac{228584\ln M}{10395}$
14	$\frac{612359\ln M}{364}-\frac{2138512657033}{787026240}$	$\frac{1218348}{1001}$	$\frac{127013964109}{82818450}-\frac{3616148\ln M}{6435}$	$\frac{99638442364}{289864575}-\frac{7043536\ln M}{45045}$
16	$\frac{967681\ln M}{135}-\frac{82365133883}{6949800}$	$\frac{965085}{182}$	$\frac{761763635183}{108216108}-\frac{2560820\ln M}{1001}$	$\frac{428362589497}{248455350}-\frac{15209336\ln M}{19305}$
18	$\frac{13741442\ln M}{459}-\frac{101648836935029}{2008492200}$	$\frac{17151277}{765}$	$\frac{58307355653567}{1895421528}-\frac{17107145\ln M}{1547}$	$\frac{184237817350667}{23455841409}-\frac{544829680\ln M}{153153}$
20	$\frac{2708773132\ln M}{21945}-\frac{272062917990438103}{1277158182300}$	$\frac{1353220726}{14535}$	$\frac{3951352873426328}{30211070175}-\frac{675640394\ln M}{14535}$	$\frac{8767893549452644}{256592689353}-\frac{1347926756\ln M}{88179}$
22	$\frac{349608740\ln M}{693}-\frac{1431681110136911151}{161325244080}$	$\frac{2795440492}{7315}$	$\frac{4624945766279214833}{845909964900}-\frac{2793108812\ln M}{14535}$	$\frac{91904978008606424}{634432473675}-\frac{2789228936\ln M}{43605}$
24	$\frac{16542939190\ln M}{8073}-\frac{3964883326088346667}{108061724370600}$	$\frac{8268943735}{5313}$	$\frac{25449328658411430081 7}{112602779739450}-\frac{132237346072\ln M}{168245}$	$\frac{2028494768572917088 37}{3356147785740 75}-\frac{264260177584\ln M}{1002915}$
26	$\frac{169660886992\ln M}{20475}-\frac{2066775856731885303313}{137034795397500}$	$\frac{84815201126}{13455}$	$\frac{16482329091591096747 19}{177793862746500}-\frac{84789942526\ln M}{26565}$	$\frac{105371053136656255554 02}{4222604240229375}-\frac{2711963087072\ln M}{2523675}$
28	$\frac{208288358800\ln M}{6237}-\frac{2760330939401667649181}{44724543113250}$	$\frac{520668477976}{20475}$	$\frac{1094517880631620904114}{28945104742125}-\frac{520577023756\ln M}{40365}$	$\frac{12274302884650696941196}{1200108573538875}-\frac{1040850944312\ln M}{239085}$
30	$\frac{1027838381233\ln M}{7656}-\frac{192323985253230982716926 83}{7642075582627200 0}$	$\frac{6166722206768}{60291}$	$\frac{37932362558490906869301}{24695627770563750}-\frac{30830570730448\ln M}{593775}$	$\frac{304519607758256513739 9176}{730284992643813 75}-\frac{61650532771376\ln M}{3511755}$
32	$\frac{81187316488225\ln M}{150722}-\frac{238617413836648281705507 6431}{23319420320602692 00}$	$\frac{16237187914229}{39556}$	$\frac{2997526345883857923005016 0013}{48195227291562351000}-\frac{389673408942436\ln M}{1869021}$	$\frac{241135852059916744112 49601813}{14239498972507058 2500}-\frac{3896357091803752\ln M}{55221075}$

Table 1.1: $a_{nm}(\ln M)$ coefficients. All the coefficients that are not explicitly shown are 0.

n	$m=0$	$m=2$	$m=4$	$m=6$
4	0	0	0	0
6	$\frac{97}{45}-\frac{4\ln M}{3}$	0	0	0
8	$\frac{1583}{105}-8\ln M$	-4	0	0
10	$\frac{10562}{135}-\frac{112\ln M}{3}$	-24	$8\ln M-\frac{8011}{315}$	0
12	$\frac{251684}{693}-160\ln M$	-112	$48\ln M-\frac{185902}{1155}$	$\frac{32\ln M}{3}-\frac{307124}{10395}$
14	$\frac{871433}{546}-660\ln M$	-480	$224\ln M-\frac{5047292}{6435}$	$64\ln M-\frac{8412904}{45045}$
16	$\frac{1835959}{270}-\frac{8008\ln M}{3}$	-1980	$960\ln M-\frac{10466956}{3003}$	$\frac{896\ln M}{3}-\frac{17570552}{19305}$
18	$\frac{21741802}{765}-\frac{32032\ln M}{3}$	-8008	$3960\ln M-\frac{45885963}{3094}$	$1280\ln M-\frac{206607056}{51051}$
20	$\frac{171608860}{1463}-42432\ln M$	-32032	$16016\ln M-\frac{59715011}{969}$	$5280\ln M-\frac{506619670}{29393}$
22	$\frac{221733355}{462}-167960\ln M$	-127296	$64064\ln M-\frac{81545956}{323}$	$\frac{64064\ln M}{3}-\frac{208425692}{2907}$
24	$\frac{5251828975}{2691}-\frac{1989680\ln M}{3}$	-503880	$254592\ln M-\frac{34489442472}{33649}$	$\frac{256256\ln M}{3}-\frac{19661441456}{66861}$
26	$\frac{53918626534}{6825}-2615008\ln M$	-1989680	$1007760\ln M-\frac{36626670967}{8855}$	$339456\ln M-\frac{1005477461344}{841225}$
28	$\frac{993906911612}{31185}-\frac{30904640\ln M}{3}$	-7845024	$3979360\ln M-\frac{670965894406}{40365}$	$1343680\ln M-\frac{1154533778012}{239085}$
30	$\frac{7363774861147}{57420}-40562340\ln M$	-30904640	$15690048\ln M-\frac{39547820883388}{593775}$	$\frac{15917440\ln M}{3}-\frac{68226557140376}{3511755}$
32	$\frac{465724831544639}{904332}-159679800\ln M$	-121687020	$61809280\ln M-\frac{248864805538 4156}{9345105}$	$20920064\ln M-\frac{4303412863931512}{55221075}$

Table 1.2: $c_{nm}(\ln M)$ coefficients. All the coefficients that are not explicitly shown are 0.

$\hat{t} \ll 1$ coefficients

NLOb

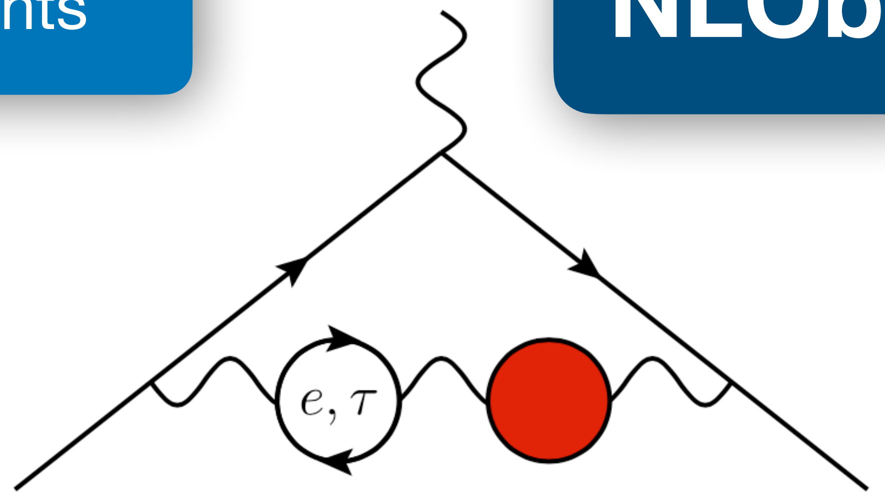

$$\sum_{\substack{n=4 \\ n\in\text{even}}}^{N}\sum_{m=0}^{M}\left[a_{nm}+b_{nm}\pi^2+c_{nm}\left(\gamma_E+\ln\hat{t}\right)+d_{nm}\left(\gamma_E+\ln\hat{t}\right)^2\right]\frac{\hat{t}^n}{n!}M^m$$

n	$m=0$	**$m=3$**	$m=4$	$m=6$
4	0	$-\frac{2}{3}$	$\frac{2}{3}$	$-\frac{4}{9}$
6	$\frac{1}{6}$	0	0	$\frac{8}{9}$
8	1	0	0	0
10	$\frac{14}{3}$	0	-1	0
12	20	0	-6	$-\frac{4}{3}$
14	$\frac{165}{2}$	0	-28	-8
16	$\frac{1001}{3}$	0	-120	$-\frac{112}{3}$
18	$\frac{4004}{3}$	0	-495	-160
20	5304	0	-2002	-660
22	20995	0	-8008	$-\frac{8008}{3}$
24	$\frac{248710}{3}$	0	-31824	$-\frac{32032}{3}$
26	326876	0	-125970	-42432
28	$\frac{3863080}{3}$	0	-497420	-167960
30	$\frac{10140585}{2}$	0	-1961256	$-\frac{1989680}{3}$
32	19959975	0	-7726160	-2615008

n	$m=0$	$m=4$	$m=6$
4	0	0	0
6	$-\frac{2}{3}$	0	0
8	-4	0	0
10	$-\frac{56}{3}$	4	0
12	-80	24	$\frac{16}{3}$
14	-330	112	32
16	$-\frac{4004}{3}$	480	$\frac{448}{3}$
18	$-\frac{16016}{3}$	1980	640
20	-21216	8008	2640
22	-83980	32032	$\frac{32032}{3}$
24	$-\frac{994840}{3}$	127296	$\frac{128128}{3}$
26	-1307504	503880	169728
28	$-\frac{15452320}{3}$	1989680	671840
30	-20281170	7845024	$\frac{7958720}{3}$
32	-79839900	30904640	10460032

Table 1.3: b_{nm} (on the left) and d_{nm} (on the right) coefficients. Notice that b_{43} is the only non-zero "odd coefficient". Again, all the coefficients that are not explicitly shown are 0.

TMR Kernels

$$\tilde{f}^{(\text{NLO}_c)}(t,\tau) = \frac{8\pi^2}{m_\mu^2}\int_0^\infty \frac{d\hat{\omega}^2}{\hat{\omega}^2}\hat{f}^{(\text{LO})}(\hat{\omega}^2)\left[\hat{\omega}^2\hat{t}^2 - 4\sin^2\frac{\hat{\omega}\hat{t}}{2}\right]\left[\hat{\omega}^2\hat{\tau}^2 - 4\sin^2\frac{\hat{\omega}\hat{\tau}}{2}\right]$$

NLOc

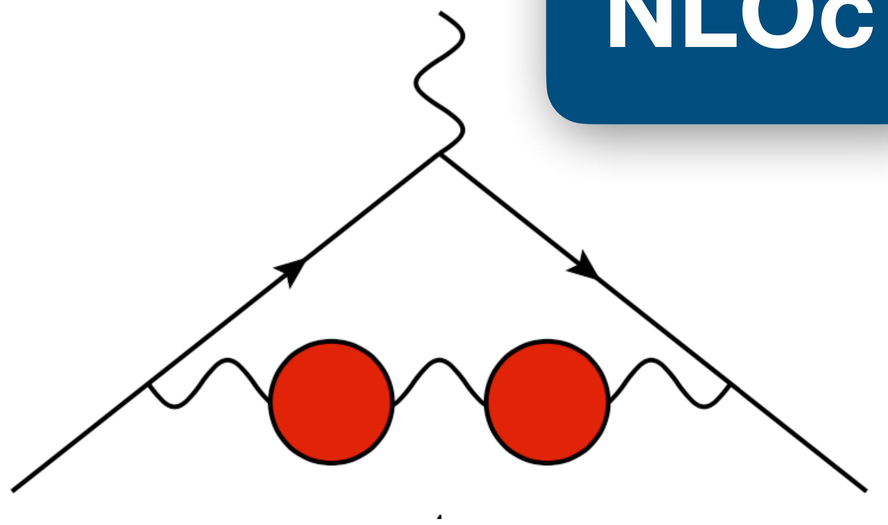

REMINDER:

$$a_\mu^{\text{hvp}}[(\text{NLO}_c)] = \left(\frac{\alpha}{\pi}\right)^3\int_0^\infty dq^2\ f^{(\text{LO})}(\hat{q}^2)\left[\hat{\Pi}(q^2)\right]^2 \Longleftarrow \hat{\Pi}(\omega^2) = \frac{4\pi^2}{\omega^2}\int_0^\infty dt\ G(t)\left[\omega^2t^2 - 4\sin^2\frac{\omega t}{2}\right]$$

Two integrals will "come out" from the Π^2 term → The Kernel for NLO_c is bi-dimensional.

$$a_\mu^{\text{hvp}}[(\text{NLO}_c)] = \left(\frac{\alpha}{\pi}\right)^3\int_0^\infty\int_0^\infty dt d\tau\ \tilde{f}^{(\text{NLO}_c)}(t,\tau)G(t)G(\tau)$$

$$\hat{\omega} = \frac{\omega}{m_\mu}$$
$$\hat{t} = m_\mu t$$
$$\hat{\tau} = m_\mu \tau$$
$$\hat{f} = m_\mu^2 f$$

$$\tilde{f}^{(\text{NLO}_c)}(t,\tau) = \frac{8\pi^2}{m_\mu^2}\int_0^\infty \frac{d\hat{\omega}^2}{\hat{\omega}^2}\hat{f}^{(\text{LO})}(\hat{\omega}^2)\left[\hat{\omega}^2\hat{t}^2 - 4\sin^2\frac{\hat{\omega}\hat{t}}{2}\right]\left[\hat{\omega}^2\hat{\tau}^2 - 4\sin^2\frac{\hat{\omega}\hat{\tau}}{2}\right]$$

NLOc

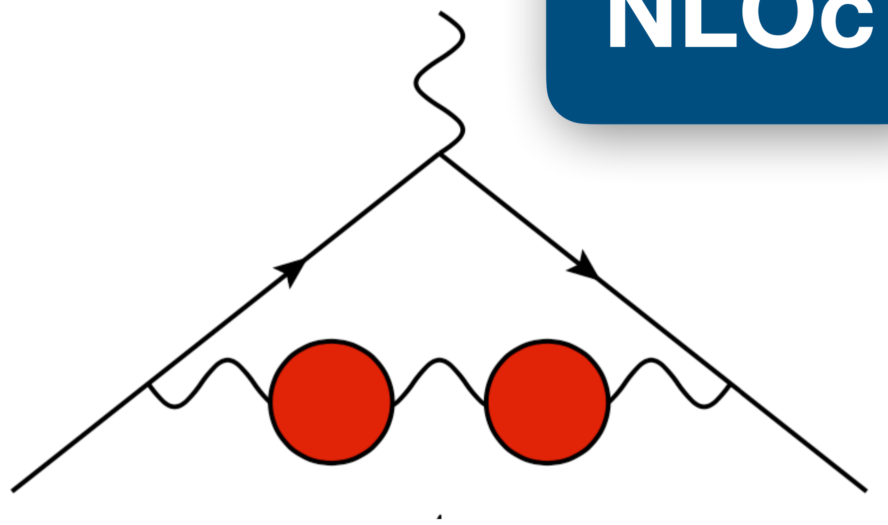

Has a closed-form solution.

The first step is to find the analytical solution:

$$\frac{m_\mu^4}{32\pi^4}\tilde{f}^{(4c)}(\hat{t},\hat{\tau}) = \frac{\hat{\tau}^2\hat{t}^2}{4} + \frac{\hat{t}^2}{\hat{\tau}^2} + \frac{\hat{\tau}^2}{\hat{t}^2} - \frac{1}{2}\left(\hat{t}^2+\hat{\tau}^2\right) + \frac{1}{6} - 2(1+\gamma_E) + 2\hat{t}^2(\ln\hat{\tau}+\gamma_E) + 2\hat{\tau}^2(\ln\hat{t}+\gamma_E) + 2\left(\hat{t}^2-1\right)\ln\hat{t} + 2\left(\hat{\tau}^2-1\right)\ln\hat{\tau}$$

$$+\left[1-(\hat{t}+\hat{\tau})^2\right]\ln(\hat{t}+\hat{\tau}) + \left[1-(\hat{t}-\hat{\tau})^2\right]\ln|\hat{t}-\hat{\tau}| + \left(\frac{\hat{t}^2}{6}-2\right)K_0(2\hat{t}) + \left(\frac{\hat{\tau}^2}{6}-2\right)K_0(2\hat{\tau}) + \left(1-\frac{1}{12}(\hat{t}+\hat{\tau})^2\right)K_0(2(\hat{t}+\hat{\tau})) + \left(1-\frac{1}{12}(\hat{t}-\hat{\tau})^2\right)K_0(2|\hat{t}-\hat{\tau}|)$$

$$-\left(\frac{2\hat{t}^2}{\hat{\tau}}+\frac{\hat{\tau}}{12}\right)K_1(2\hat{\tau}) - \left(\frac{2\hat{\tau}^2}{\hat{t}}+\frac{\hat{t}}{12}\right)K_1(2\hat{t}) + \frac{1}{24}|\hat{t}-\hat{\tau}|K_1(2|\hat{t}-\hat{\tau}|) + \frac{1}{24}(\hat{t}+\hat{\tau})K_1(2(\hat{t}+\hat{\tau})) + \left(\frac{\hat{t}^2}{12}+\frac{\hat{\tau}^2}{4}-\frac{15}{16}\right)G_{1,3}^{2,1}\left(\hat{t}^2\,\middle|\,\begin{matrix}\frac{3}{2}\\ 0,1,\frac{1}{2}\end{matrix}\right)$$

$$+\left(\frac{\hat{\tau}^2}{12}+\frac{\hat{t}^2}{4}-\frac{15}{16}\right)G_{1,3}^{2,1}\left(\hat{\tau}^2\,\middle|\,\begin{matrix}\frac{3}{2}\\ 0,1,\frac{1}{2}\end{matrix}\right) + \left(\frac{15}{32}-\frac{1}{24}(\hat{t}+\hat{\tau})^2\right)G_{1,3}^{2,1}\left((\hat{t}+\hat{\tau})^2\,\middle|\,\begin{matrix}\frac{3}{2}\\ 0,1,\frac{1}{2}\end{matrix}\right) + \left(\frac{15}{32}-\frac{1}{24}(\hat{t}-\hat{\tau})^2\right)G_{1,3}^{2,1}\left((\hat{t}-\hat{\tau})^2\,\middle|\,\begin{matrix}\frac{3}{2}\\ 0,1,\frac{1}{2}\end{matrix}\right)$$

TMR Kernels

$$\tilde{f}^{(\mathrm{NLO_c})}(t,\tau) = \frac{8\pi^2}{m_\mu^2}\int_0^\infty \frac{d\hat{\omega}^2}{\hat{\omega}^2}\hat{f}^{(\mathrm{LO})}(\hat{\omega}^2)\left[\hat{\omega}^2\hat{t}^2 - 4\sin^2\frac{\hat{\omega}\hat{t}}{2}\right]\left[\hat{\omega}^2\hat{\tau}^2 - 4\sin^2\frac{\hat{\omega}\hat{\tau}}{2}\right]$$

NLOc

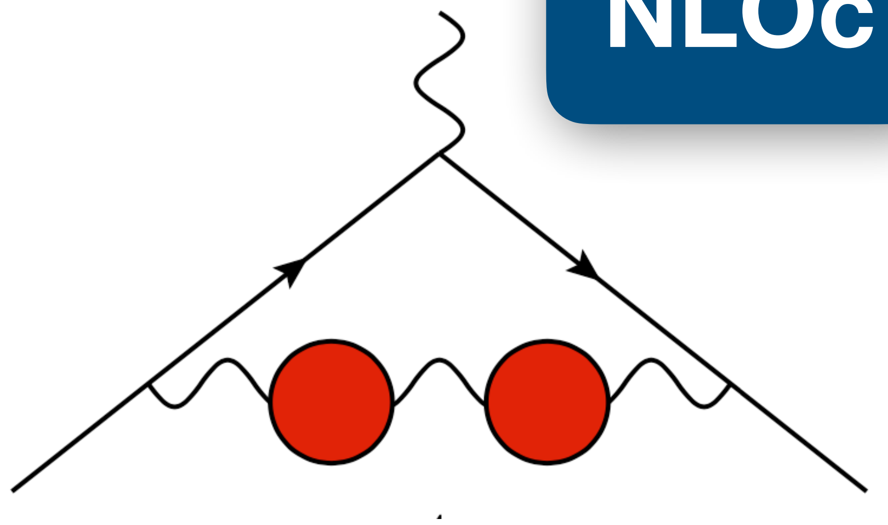

Has a closed-form solution.

The first step is to find the analytical solution:

$$\frac{m_\mu^4}{32\pi^4}\tilde{f}^{(4c)}(\hat{t},\hat{\tau}) = \frac{\hat{\tau}^2\hat{t}^2}{4} + \frac{\hat{t}^2}{\hat{\tau}^2} + \frac{\hat{\tau}^2}{\hat{t}^2} - \frac{1}{2}\left(\hat{t}^2+\hat{\tau}^2\right) + \frac{1}{6} - 2(1+\gamma_E) + 2\hat{t}^2(\ln\hat{\tau}+\gamma_E) + 2\hat{\tau}^2(\ln\hat{t}+\gamma_E) + 2\left(\hat{t}^2-1\right)\ln\hat{t} + 2\left(\hat{\tau}^2-1\right)\ln\hat{\tau}$$

$$+\left[1-(\hat{t}+\hat{\tau})^2\right]\ln(\hat{t}+\hat{\tau}) + \left[1-(\hat{t}-\hat{\tau})^2\right]\ln|\hat{t}-\hat{\tau}| + \left(\frac{\hat{t}^2}{6}-2\right)K_0(2\hat{t}) + \left(\frac{\hat{\tau}^2}{6}-2\right)K_0(2\hat{\tau}) + \left(1-\frac{1}{12}(\hat{t}+\hat{\tau})^2\right)K_0(2(\hat{t}+\hat{\tau})) + \left(1-\frac{1}{12}(\hat{t}-\hat{\tau})^2\right)K_0(2|\hat{t}-\hat{\tau}|)$$

$$-\left(\frac{2\hat{t}^2}{\hat{\tau}}+\frac{\hat{\tau}}{12}\right)K_1(2\hat{\tau}) - \left(\frac{2\hat{\tau}^2}{\hat{t}}+\frac{\hat{t}}{12}\right)K_1(2\hat{t}) + \frac{1}{24}|\hat{t}-\hat{\tau}|K_1(2|\hat{t}-\hat{\tau}|) + \frac{1}{24}(\hat{t}+\hat{\tau})K_1(2(\hat{t}+\hat{\tau})) + \left(\frac{\hat{t}^2}{12}+\frac{\hat{\tau}^2}{4}-\frac{15}{16}\right)G_{1,3}^{2,1}\left(\hat{t}^2\,\middle|\,\begin{matrix}\frac{3}{2}\\ 0,1,\frac{1}{2}\end{matrix}\right)$$

$$+\left(\frac{\hat{\tau}^2}{12}+\frac{\hat{t}^2}{4}-\frac{15}{16}\right)G_{1,3}^{2,1}\left(\hat{\tau}^2\,\middle|\,\begin{matrix}\frac{3}{2}\\ 0,1,\frac{1}{2}\end{matrix}\right) + \left(\frac{15}{32}-\frac{1}{24}(\hat{t}+\hat{\tau})^2\right)G_{1,3}^{2,1}\left((\hat{t}+\hat{\tau})^2\,\middle|\,\begin{matrix}\frac{3}{2}\\ 0,1,\frac{1}{2}\end{matrix}\right) + \left(\frac{15}{32}-\frac{1}{24}(\hat{t}-\hat{\tau})^2\right)G_{1,3}^{2,1}\left((\hat{t}-\hat{\tau})^2\,\middle|\,\begin{matrix}\frac{3}{2}\\ 0,1,\frac{1}{2}\end{matrix}\right)$$

TMR Kernels

NLOc

$$\tilde{f}^{(\text{NLO}_c)}(t,\tau) = \frac{8\pi^2}{m_\mu^2}\int_0^\infty \frac{d\hat{\omega}^2}{\hat{\omega}^2}\hat{f}^{(\text{LO})}(\hat{\omega}^2)\left[\hat{\omega}^2\hat{t}^2 - 4\sin^2\frac{\hat{\omega}\hat{t}}{2}\right]\left[\hat{\omega}^2\hat{\tau}^2 - 4\sin^2\frac{\hat{\omega}\hat{\tau}}{2}\right]$$

Similar procedure as before

- We expand for $\hat{t}, \hat{\tau} \ll 1$ in the green region.
- We expand for $\hat{t}, \hat{\tau}, \hat{t}+\hat{\tau}, |\hat{t}-\hat{\tau}| \gg 1$ in the blue region.
- Exp. suppressed terms are expanded around $\hat{t}_0 = \hat{\tau}_0 = T_0 = 2.2$ to interpolate both limit expansions.
  $$\propto e^{-2\hat{t}},\ e^{-2\hat{\tau}},\ e^{-2(\hat{t}+\hat{\tau})},\ e^{-2(\hat{t}-\hat{\tau})}$$
- For the red region, the asymptotic expansion from terms with $\hat{t}-\hat{\tau}$ dependence is subtracted and expanded around $\hat{t}-\hat{\tau} \ll 1$.
- For the yellow region, the asymptotic expansion from terms with $\hat{t}$ ($\hat{\tau}$) dependence is subtracted and expanded around $\hat{t} \ll 1$ ($\hat{\tau} \ll 1$).

By a correct choice of the region limits and by computing terms up to $N = 30$ and $P = 13$ for $T_0 = 2.2$ a precision $< 10^{-8}\ \forall\ \hat{t},\ \hat{\tau}$ has been achieved.

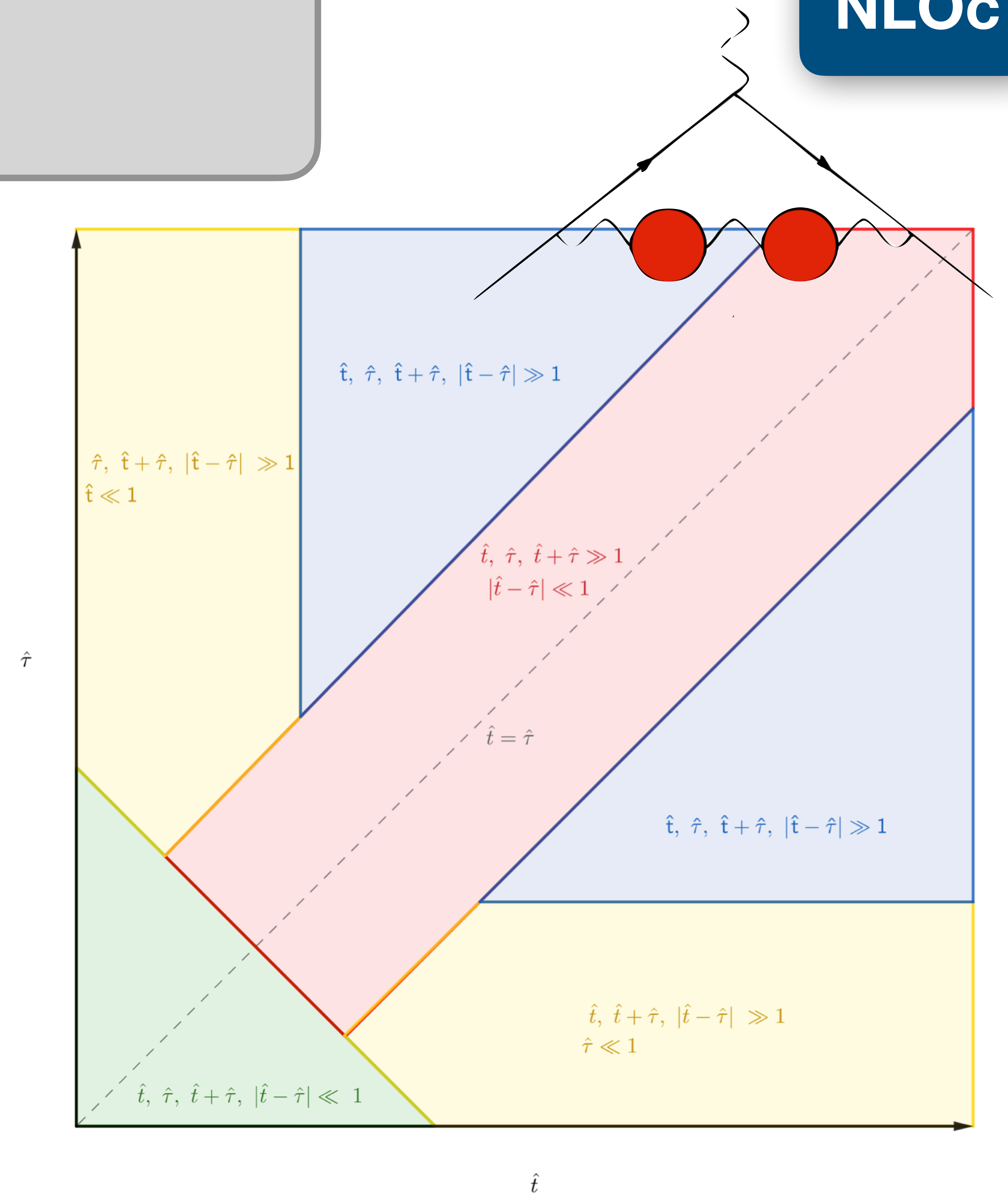

$$\tilde{f}^{(\text{NLO}_c)}(t,\tau) = \frac{8\pi^2}{m_\mu^2}\int_0^\infty \frac{d\hat{\omega}^2}{\hat{\omega}^2}\hat{f}^{(\text{LO})}(\hat{\omega}^2)\left[\hat{\omega}^2\hat{t}^2 - 4\sin^2\frac{\hat{\omega}\hat{t}}{2}\right]\left[\hat{\omega}^2\hat{\tau}^2 - 4\sin^2\frac{\hat{\omega}\hat{\tau}}{2}\right]$$

NLOc

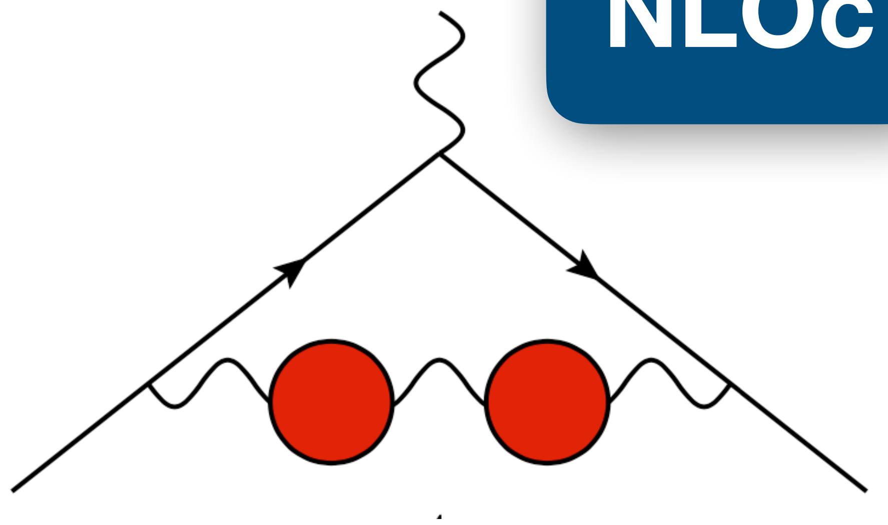

Expansion for the green region:

$$\frac{m_\mu^4}{32\pi^4}\tilde{f}^{(\text{NLO}_c)}(\hat{t},\hat{\tau}) = \sum_{\substack{n=4 \\ n\in\text{even}}}^{N}\left[\frac{a_n^{(2)}}{n!}\left(\hat{t}^2\hat{\tau}^n + \hat{\tau}^2\hat{t}^n\right) + \frac{b_n^{(2)}}{n!}\left(\hat{t}^2(\gamma_E + \ln\hat{\tau})\hat{\tau}^n + \hat{\tau}^2(\gamma_E + \ln\hat{t})\hat{t}^n\right)\right.$$

$$+2\sum_{\substack{n=6 \\ n\in\text{even}}}^{N}\left[\frac{a_n^{(3)}}{n!}\left((\hat{t}+\hat{\tau})^n + (\hat{t}-\hat{\tau})^n - 2\hat{\tau}^n - 2\hat{t}^n\right)\right.$$

$$\left.+\frac{b_n^{(3)}}{n!}\left((\gamma_E + \ln(\hat{t}+\hat{\tau}))(\hat{t}+\hat{\tau})^n + (\gamma_E + \ln|\hat{t}-\hat{\tau}|)(\hat{t}-\hat{\tau})^n - 2(\gamma_E + \ln\hat{t})\hat{\tau}^n - 2(\gamma_E + \ln\hat{\tau})\hat{t}^n\right)\right]$$

n	$a_n^{(2)}$	$b_n^{(2)}$	$a_n^{(3)}$	$b_n^{(3)}$
0	0	0	$-\frac{11}{24} - \frac{\ln 2}{2}$	0
2	$-\frac{1}{2}$	0	$-\frac{5}{4} + \ln 2$	0
4	$\frac{1}{3}$	0	$\frac{1}{4}$	0
6	$-\frac{169}{60}$	2	$-\frac{1}{6}$	0
8	$-\frac{802}{35}$	12	$\frac{176}{105}$	-1
10	$-\frac{5509}{45}$	56	$\frac{1336}{105}$	-6
12	$-\frac{44118}{77}$	240	$\frac{65429}{990}$	-28
14	$-\frac{1837077}{728}$	990	$\frac{304587}{1001}$	-120
16	$-\frac{967681}{90}$	4004	$\frac{965085}{728}$	-495
18	$-\frac{6870721}{153}$	16016	$\frac{17151277}{3060}$	-2002
20	$-\frac{1354386566}{7315}$	63648	$\frac{676610363}{29070}$	-8008
22	$-\frac{174804370}{231}$	251940	$\frac{698860123}{7315}$	-31824
24	$-\frac{8271469595}{2691}$	994840	$\frac{8268943735}{21252}$	-125970
26	$-\frac{84830443496}{6825}$	3922512	$\frac{42407600563}{26910}$	-497420
28	$-\frac{104144179400}{2079}$	15452320	$\frac{130167119494}{20475}$	-1961256
30	$-\frac{1027838381233}{5104}$	60843510	$\frac{1541680551692}{60291}$	-7726160

Table 1.4: Small distance expansion coefficients $a_n^{(2)}$, $b_n^{(2)}$, $a_n^{(3)}$ and $b_n^{(3)}$.

By a correct choice of the region limits and by computing terms up to $N = 30$ and $P = 13$ for $T_0 = 2.2$ a precision $< 10^{-8}\ \forall\ \hat{t}, \hat{\tau}$ has been achieved.

Procedure and CLS ensembles

Now we are ready to combine our NLO Kernels with $G(t)$ from the lattice simulations.

- For this analysis, so far 12 different CLS ensembles with $N_f = 2 + 1$ flavors, different lattice spacing, pion, and kaon masses have been used.

$$G(t) = G(t; a, V, m_\pi, m_k)$$

To quote an estimation of $a_\mu^{\rm hvp}$ at the physical point:

M. T. Hansen & A. Patella. 2019 . Finite-volume effects in $(g-2)^{\rm HVP,LO}$

- $V \to \infty$
- $a \to 0$
- $m_\pi \to m_\pi^{\rm ph}$
- $m_k \to m_k^{\rm ph}$

- V has been corrected through the Hansen-Patela method
- a, m_π, m_k are extrapolated to their physical value

Since Gérardin et al., 1904.03120

- New Ensemble
- Significantly improved statistics

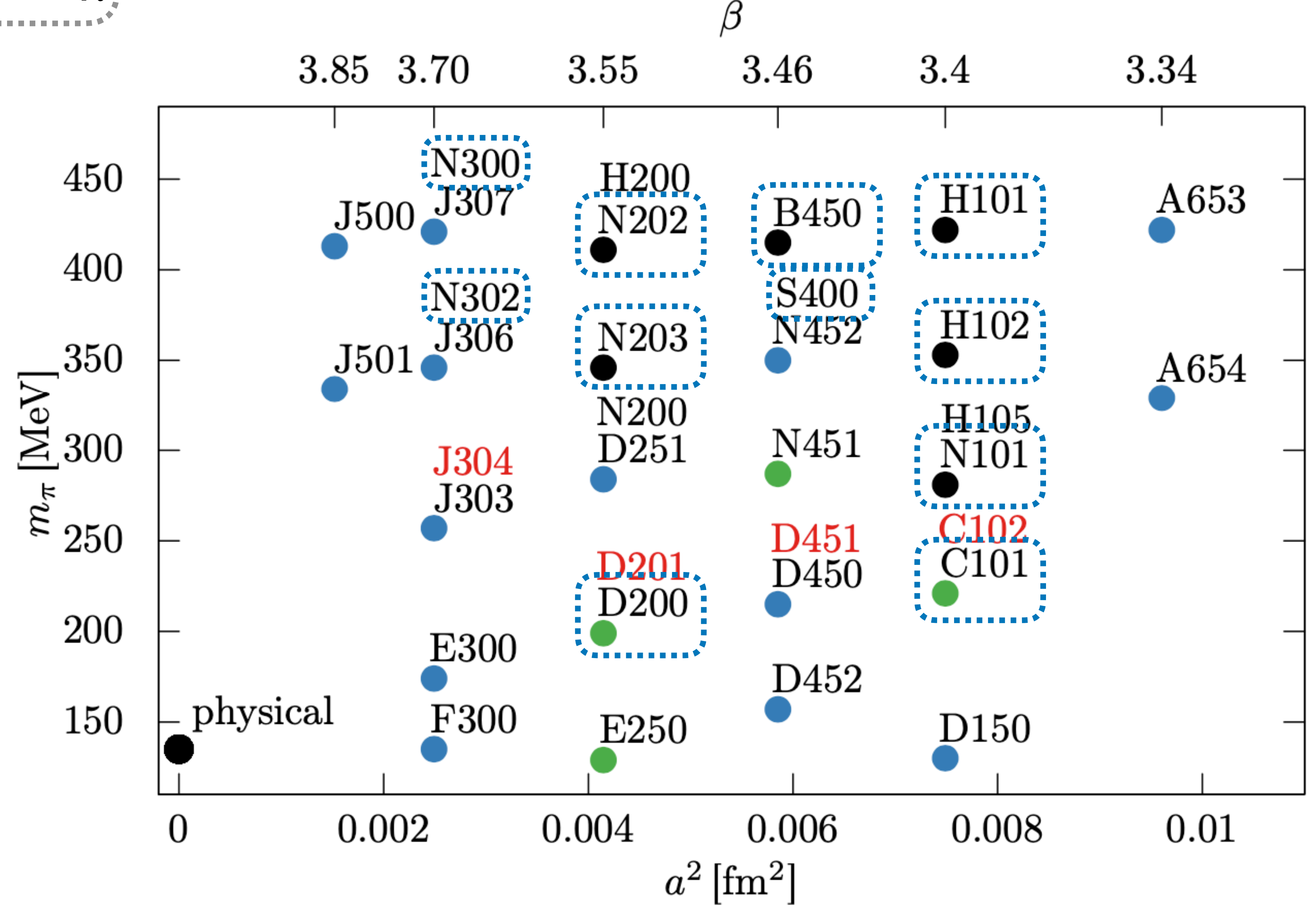

Isospsin basis

It is convenient to work on the isospin basis

Isosvector Isoscalar

$$j_\mu^{\text{em}} = \frac{2}{3}\bar{u}\gamma_\mu u - \frac{1}{3}\bar{d}\gamma_\mu d - \frac{1}{3}\bar{s}\gamma_\mu s + \frac{2}{3}\bar{c}\gamma_\mu c + \ldots = j_\mu^3 + \frac{1}{\sqrt{3}} j_\mu^8 + \frac{2}{3}\bar{c}\gamma_\mu c + \ldots$$

Contributions coming from the $\ldots$ correspond to contributions from the bottom and top which are neglected.

This description will give place to some mixing between the currents in the full correlator:

$$G = -\frac{1}{3}\sum_{\vec{x}\in\Lambda}\langle j_\mu^{em} j_\mu^{em}\rangle = G^{33} + \frac{1}{3}G^{88} + \frac{4}{9}G^{cc}_{\text{conn}} + \frac{2}{3\sqrt{3}}G^{c8}_{\text{disc}} + \frac{4}{9}G^{cc}_{\text{disc}} + \ldots$$

$SU_F(3) + 1/m_c$ suppression → negligible

- $G^{33} = \frac{1}{2}G^{ll}_{\text{conn}}$
- $G^{88} = \frac{1}{6}\left[G^{ll}_{\text{conn}} + 2G^{ss}_{\text{conn}} + 2G^{88}_{\text{disc}}\right]$

$$G \times G \approx G^{33}G^{33} + \frac{1}{9}G^{88}G^{88} + \frac{16}{81}G^{cc}_{\text{conn}}G^{cc}_{\text{conn}} + \frac{2}{3}G^{33}G^{88} + \frac{8}{9}G^{33}G^{cc}_{\text{conn}} + \frac{8}{27}G^{88}G^{cc}_{\text{conn}}$$

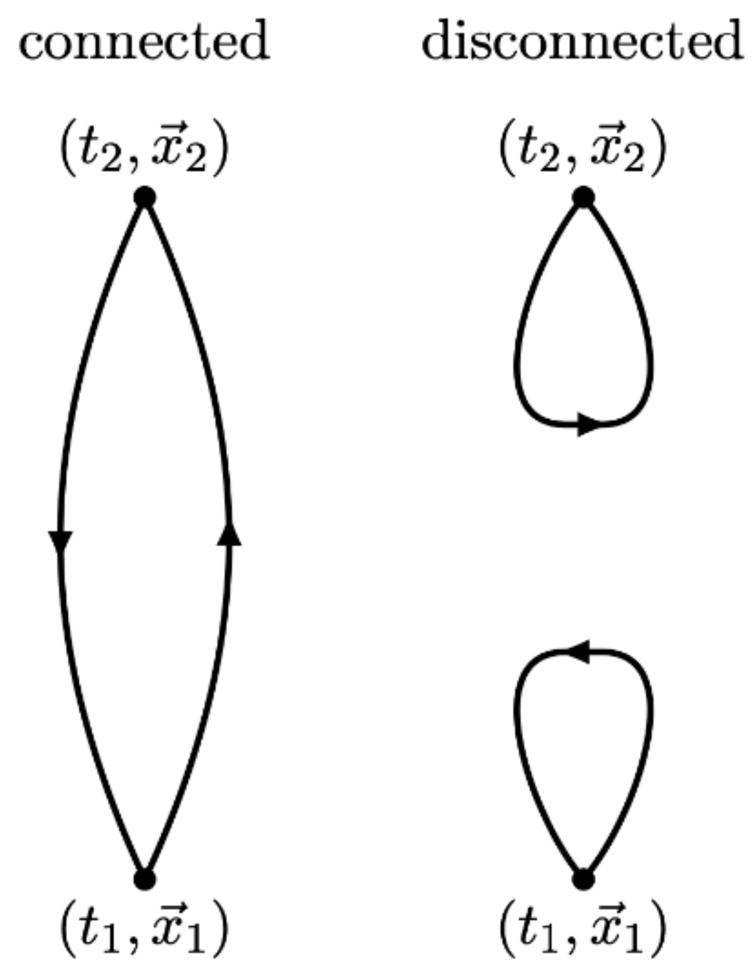

Isospsin basis

$$G = -\frac{1}{3}\sum_{\vec{x}\in\Lambda}\langle j_\mu^{em} j_\mu^{em}\rangle = G^{33} + \frac{1}{3}G^{88} + \dots$$

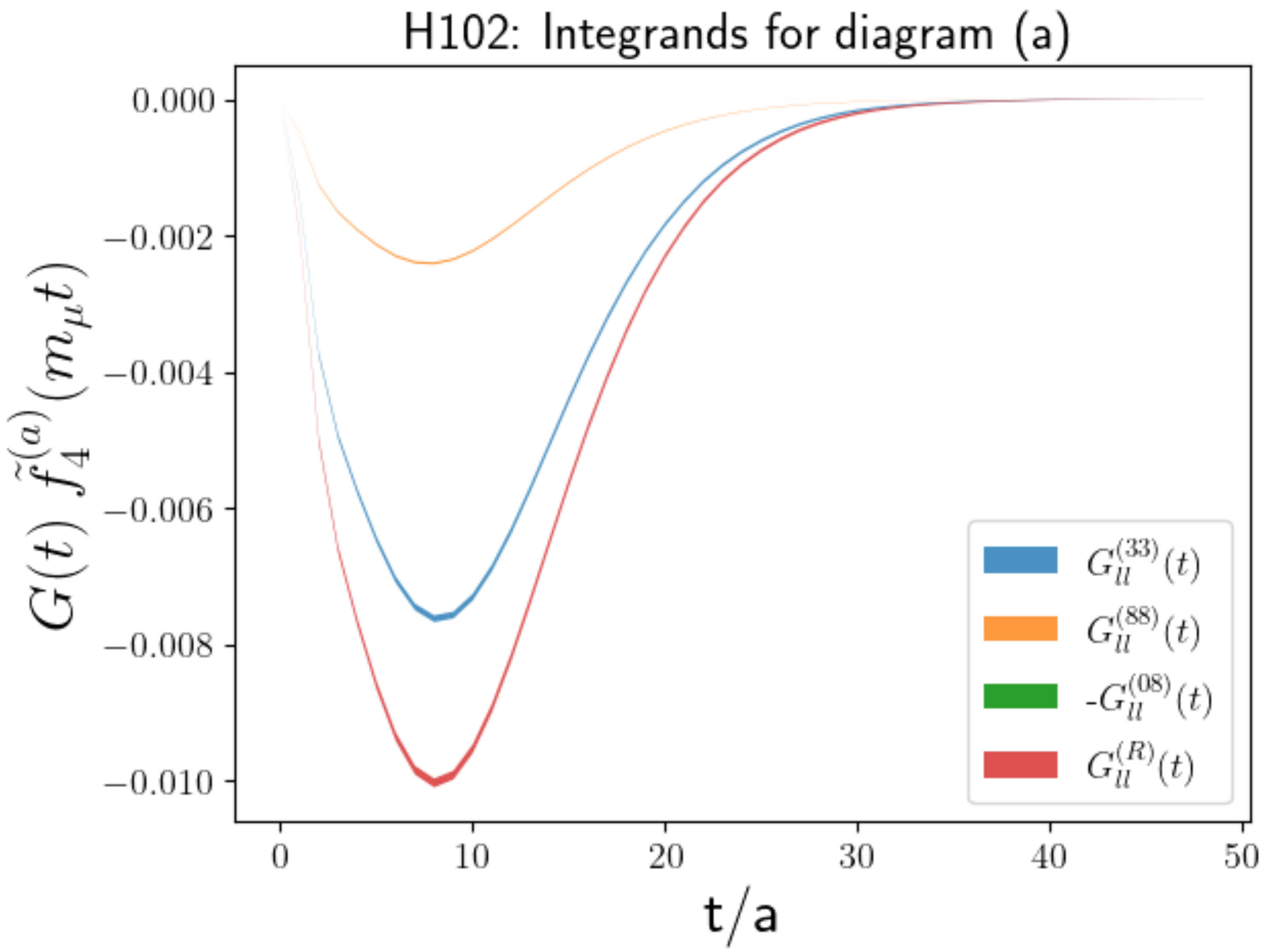

$\mathcal{O}(a)$ improvement and current descriptions

- Two different current discretizations have been used, local-local and local-conserved correlators will be used in the extrapolation (conserved currents are normalized by construction)

$$j_\mu^{(L),a}(x) = \overline{\psi}(x)\gamma_\mu T^a \psi(x)$$

$$j_\mu^{(C),a}(x) = \frac{1}{2}\left(\overline{\psi}(x+a\hat{\mu})(1+\gamma_\mu)U_\mu^\dagger(x)T^a\psi(x) - \overline{\psi}(x)(1-\gamma_\mu)U_\mu(x)T^a\psi(x+a\hat{\mu})\right)$$

- Currents are also improved to $\mathcal{O}(a)$ following two different Symanzik improvement programs which differ only at $\mathcal{O}(a^2)$, we will refer to these as “Set 1” and “Set 2”.

$$j_\mu^{(\alpha),a}(x) \sim \mathcal{O}(a)$$

$$j_\mu^{(\alpha),a,I(\text{set})}(x) = j_\mu^{(\alpha),a}(x) + c_v^{(\text{set})}\tilde{\partial}_\nu \left(-\frac{1}{2}\overline{\psi}(x)\left[\gamma_\mu,\gamma_\nu\right]\frac{\lambda^a}{2}\psi(x)\right) \sim \mathcal{O}(a^2)$$

Physical point extrapolation
Model average

NLO computation

$$(a, m_\pi, m_k) \longrightarrow (0, m_\pi^{\rm ph}, m_k^{\rm ph})$$

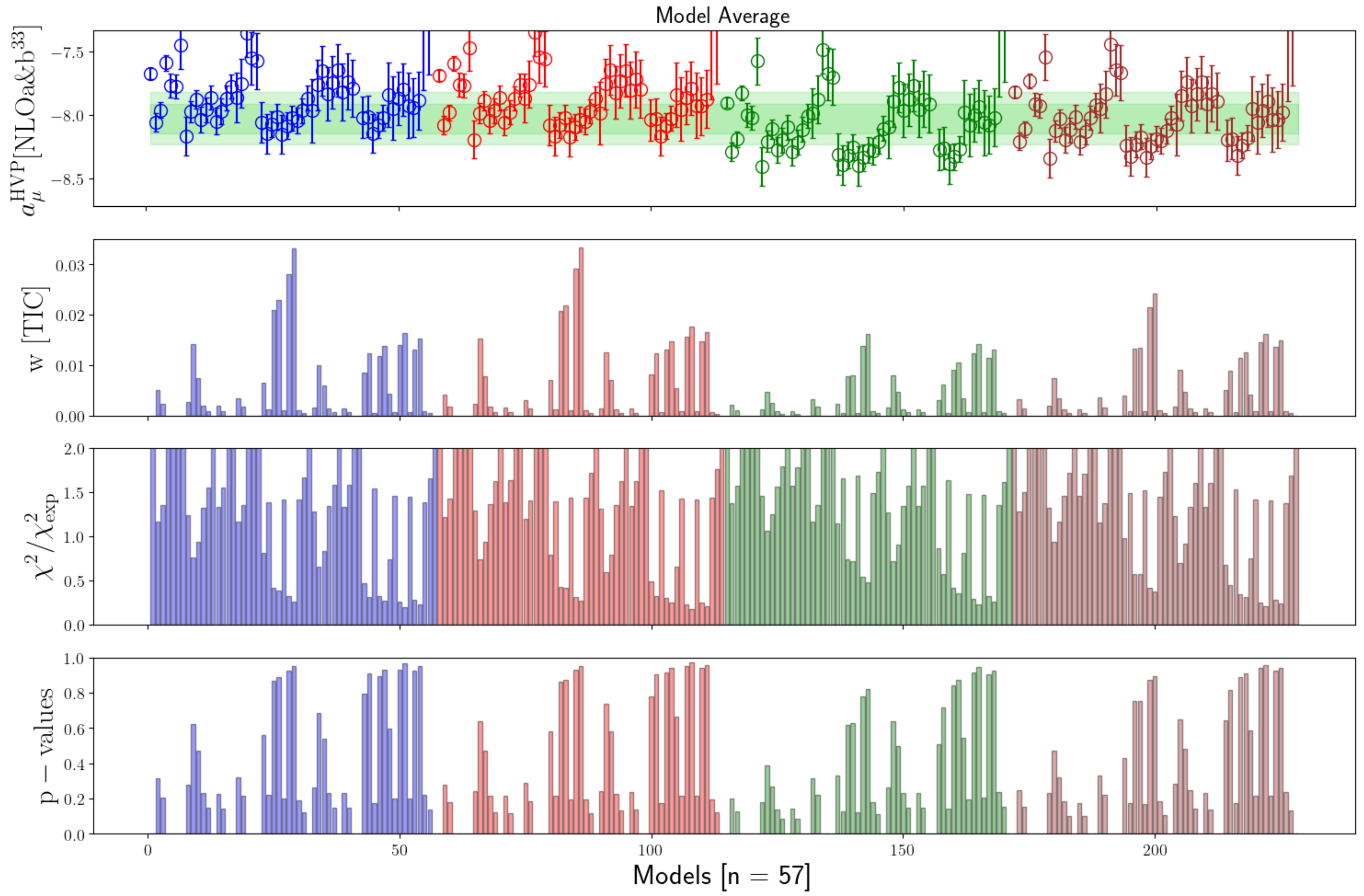

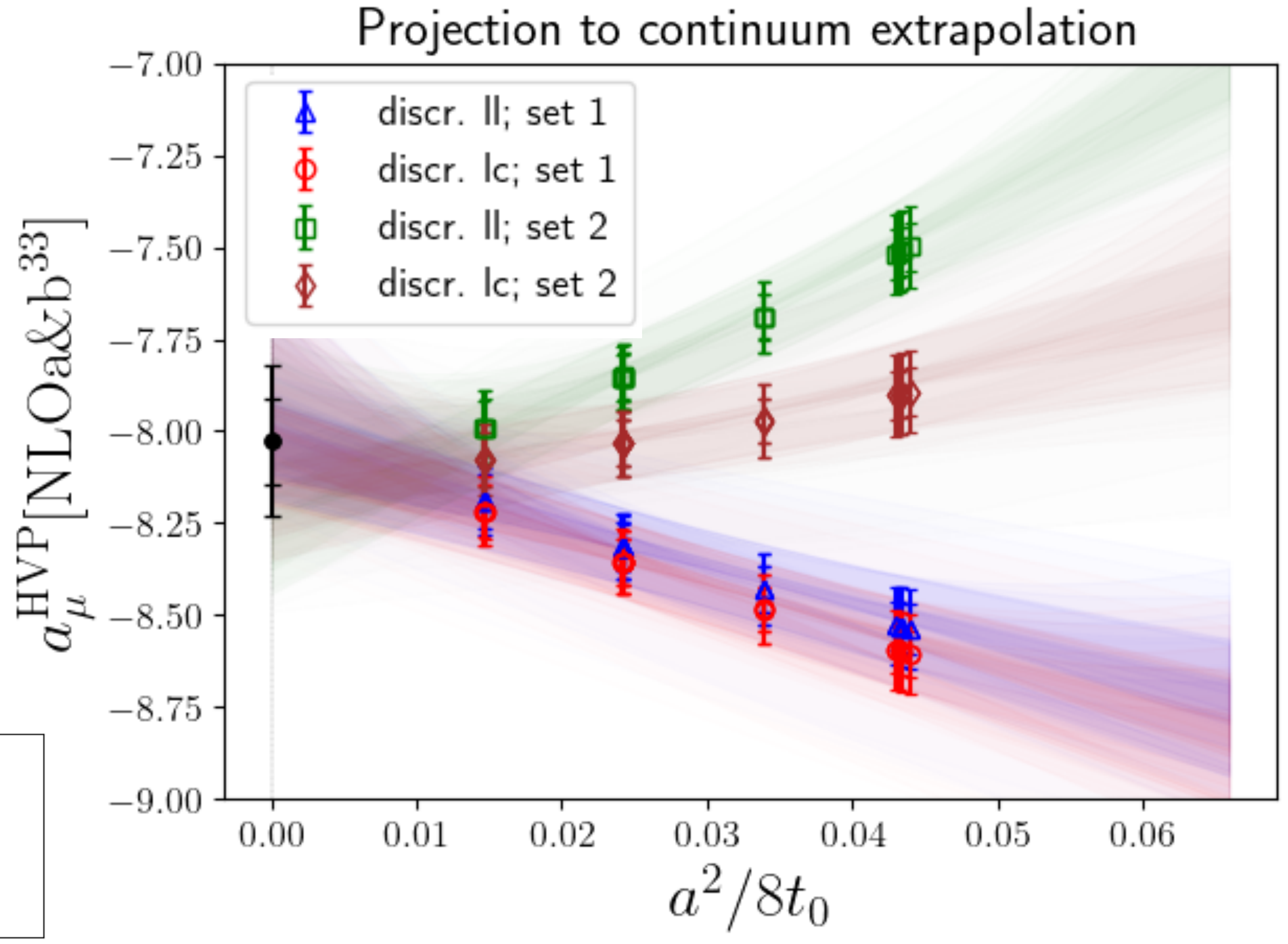

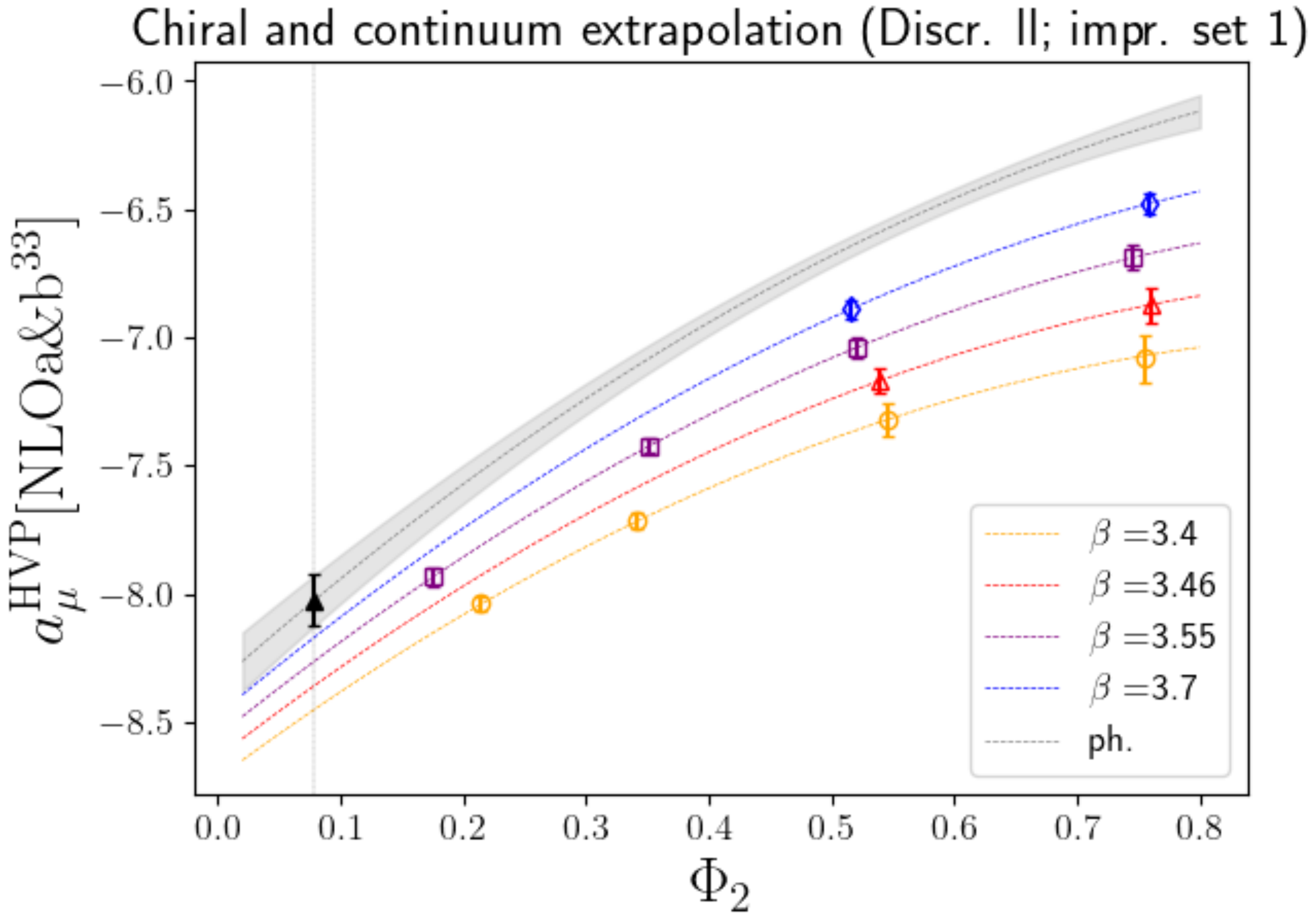

$$a_\mu^{\rm hvp}(a, m_\pi, m_k) = a_\mu^{\rm hvp} + \alpha\chi_a + \beta\left(\phi_2 - \phi_2^{ph}\right) + \gamma\left(\phi_4 - \phi_4^{ph}\right) + \begin{cases} \phi_2^2 - \left(\phi_2^{ph}\right)^2 \\ \chi_a\left(\phi_2 - \phi_2^{ph}\right) \\ \chi_a\left(\phi_4 - \phi_4^{ph}\right) \\ \dots \end{cases}$$

Base model

Permuted terms

$$\chi_a = \frac{a^2}{8t_0}, \quad \phi_2 = 8t_0 m_\pi^2, \quad \phi_4 = 8t_0\left(m_k^2 + \frac{1}{2}m_\pi^2\right)$$

Preliminary results

$$a_\mu^{\rm hvp}[{\rm NLO_a}] = -16.60(37)(55) + \frac{1}{3}[-10.33(27)(51)] + \frac{4}{9}[-1.986(26)(78) + 67.0(0.0)(7.0)\times 10^{-5}] + \frac{2}{3\sqrt{3}}[3.0(6.0)(2.0)\times 10^{-5}] = \mathbf{-20.92(42)(57)} \quad [3.38\%]$$

$$a_\mu^{\rm hvp}[{\rm NLO_b}] = 8.64(25)(34) + \frac{1}{3}[4.83(19)(29)] + \frac{4}{9}[0.556(07)(22) - 20.2(0.0)(5.7)\times 10^{-5}] + \frac{2}{3\sqrt{3}}[-1.6(4.0)(4.4)\times 10^{-5}] = \mathbf{10.49(28)(35)} \quad [4.27\%]$$

➡ $$a_\mu^{\rm hvp}[{\rm NLO_{a\&b}}] = -7.96(13)(19) + \frac{1}{3}[-5.50(10)(22)] + \frac{4}{9}[-1.430(16)(56) + 47(22)(12)\times 10^{-5}] + \frac{2}{3\sqrt{3}}[1.7(5.9)(7.2)\times 10^{-5}] = \mathbf{-10.43(15)(21)} \quad [2.47\%]$$

➡ $$a_\mu^{\rm hvp}[{\rm NLO_c}] = 0.226(09)(12) + \frac{1}{9}[0.0810(52)(87)] + \frac{16}{81}[0.00213(50)(17)] + \frac{2}{3}[0.1253(60)(95)] + \frac{8}{9}[0.0180(05)(10)] + \frac{8}{27}[0.0087(19)(38)] = \mathbf{0.338(13)(14)} \quad [5.65\%]$$

$$a_\mu^{\rm hvp}[{\rm NLO}] = a_\mu^{\rm hvp}[{\rm NLO_{a\&b}}] + a_\mu^{\rm hvp}[{\rm NLO_c}] = \mathbf{-10.10(14)(21)} = \mathbf{-10.10(25)} \quad [2.50\%]$$

up to $\times 10^{-10}$

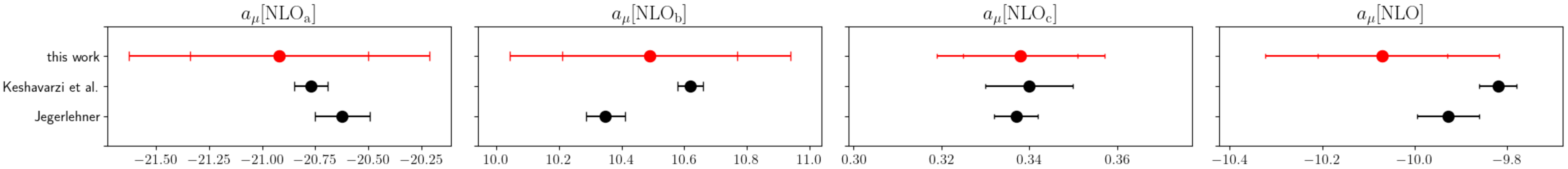

Agreement between lattice and data-driven determinations at this stage of precision. Future plans include an increase in the lattice phase space which will severely improve the extrapolation, hopefully achieving an increase in precision by a factor $\gtrsim 3$.

Conclusions and outlook

- NLO electromagnetic corrections to the HVP can be computed in the lattice, these, will become relevant in the full lattice HVP estimation as different collaborations keep pushing for precision.
- This computation provides a new tool to prove lattice vs data-driven approaches.
- Already at this stage, a $2.5\ \%$ precession can be obtained. NLO may be naturally more precise than the LO computation.
- Next step, include full CLS ensembles and statics to increase precision to sub-percent accuracy.
- Improved bounding method and other Finite-Volume correctors will be studied. As well as corrections for the charm mass miss-tuning.
- Blinding analysis to avoid unconscious bias.

Extra slides

a_μ^{hvp} from data driven | a_μ^{hvp} from lattice simulations

$\hat{\Pi}(q^2)$ **must** be found non-perturbatively.

Analyticity and the **optical theorem** allow rewriting the HVP as the cross-section of a well-known process: $e^+e^- \to \text{hadrons}$ (or $\tau \to \text{hadrons} + \nu$).

$$\hat{\Pi}(q^2) = \frac{q^2}{3}\int_{s_{th}}^{\infty} ds \frac{R(s)}{s(s+q^2)}$$

$$R(s) = \frac{\sigma\left(e^+e^- \to \text{hadrons}\right)}{4\pi\alpha^2/s}$$

So a_μ^{hvp} is rewritten in the following form:

$$a_\mu^{\text{hvp}}[(i)] = \left(\frac{\alpha}{\pi}\right)^{\geq 2} \int_{s_{\text{th}}}^{\infty} \frac{ds}{s} K^{(i)}(s) R(s)$$

$$K^{(i)}(s) = \frac{1}{3}\int_0^{\infty} d\hat{q}^2 \; \hat{f}^{(i)}(\hat{q}^2) \frac{\hat{q}^2}{\hat{s}+\hat{q}^2}$$

$\hat{q} = \frac{q}{m_\mu}$
$\hat{f} = m_\mu^2 f$

$\sigma(e^+e^- \to \pi^+\pi^-)$

Alex Kashevarzi, KNTW:Data-Driven HVP, 7^{th} plenary workshop muon g-2